Sigma-Point Kalman Filtering for Integrated GPS and Inertial Navigation

John L. Crassidis*

University at Buffalo, State University of New York, Amherst, NY 14260-4400

A sigma-point Kalman filter is derived for integrating GPS measurements with inertial measurements from gyros and accelerometers to determine both the position and the attitude of a moving vehicle. Sigma-point filters use a carefully selected set of sample points to more accurately map the probability distribution than the linearization of the standard extended Kalman filter, leading to faster convergence from inaccurate initial conditions in position/attitude estimation problems. The filter formulation is based on standard inertial navigation equations. The global attitude parameterization is given by a quaternion, while a generalized three-dimensional attitude representation is used to define the local attitude error. A multiplicative quaternion-error approach is used to guarantees that quaternion normalization is maintained in the filter. Simulation results are shown to compare the performance of the sigma-point filter with a standard extended Kalman filter approach.

I. Introduction

The integration of Global Positioning System (GPS) signals with Inertial Measurement Units (IMUs) has become a standard approach for position and attitude determination of a moving vehicle. An Inertial Navigation System (INS) is best described in the Preface section of the excellent book by Chatfield,[1] who states "Inertial navigation involves a blend of inertial measurements, mathematics, control system design, and geodesy." Historically, INS's were primarily used for military and commercial aircraft applications due to their high cost. However, with the advent of cheaper sensors, especially micro-mechanical ones,[2] several new applications have become mainstream, including uninhabited air vehicles, micro-robots, and even guided munitions.† Although these cheaper sensors do not perform as well as high-grade sensors in terms of drift and white-noise measurement errors, they can be used to meet the requirements of several vehicle position/attitude knowledge specifications when aided with GPS. This allows for an attractive approach since a completely self-contained system can be used to calibrate IMUs online using GPS-determined position observations, while also determining vehicle attitude and rates in realtime.

By far the primary mechanism historically used to blend GPS measurements with IMU data has been the extended Kalman filter (EKF).[3] There are many approaches to mechanize an integrated GPS/INS in an EKF though. One aspect involves how GPS observations are used in the filter design. The term "loosely-coupled" is used to signify that position estimates taken from the GPS are used in the EKF as measurements, while a "tightly-coupled" configuration utilizes the GPS pseudoranges directly. The main advantage of a tightly-coupled system is that state quantity estimates can still be provided even when the minimum number of four GPS satellites is not available. However, a tightly-coupled system requires knowledge of variables used to implement the tracking loops that may not be readily available. Another aspect of an integrated GPS/INS is the coordinate system used to described the determined position and attitude. The Earth-Centered-Earth-Fixed (ECEF) frame, which will be described later, is useful since GPS receivers typically calculate positions in this frame directly. However, the attitude of an air or ground vehicle is not physical intuitive in this frame which is why a local frame, such as the North-East-Down (NED) frame, is often used. Also, since a linearization of the equations of motion is required for the EKF, then using one frame over another can produce different overall performance characteristics. For example, for long duration navigation, the local

*Associate Professor, Department of Mechanical & Aerospace Engineering. Email: johnc@eng.buffalo.edu. Associate Fellow AIAA.

†See http://www.airpower.maxwell.af.mil/airchronicles/cc/pinker.html for recent contributions of GPS/INS to Air Force competencies.

NED frame separates the unstable vertical axis from the more stable horizontal axes which provides more intuitive schemes for analyzing INS errors than using the ECEF frame.[4] The conversions between various frames is well known (see Ref. 1 for more details). However, mapping of the covariance of the errors has not been seen by the present author. Therefore, one of the goals of this paper is to present covariance mappings between the NED and ECEF frames.

The EKF is widely used in practice, but it has one well-known drawback. If the errors are not within the "linear region", then filter divergence may occur. This is especially a problem for an integrated GPS/INS since, even though position is well known, attitude and IMU calibration parameters may not be well known *a prior*. In fact to this day the most researched topic in INS's has been initial alignment and attitude determination.[1] Sigma-point Kalman filters essentially provide derivative-free higher-order approximations by approximating a Gaussian distribution rather than approximating an arbitrary nonlinear function as the EKF does.[5] They can provide more accurate results than an EKF, especially when accurate initial condition states are not well known. A sigma-point GPS/INS filter has been presented in Ref. 6, which also includes a method to fuse latency lagged observations in a theoretically consistent fashion. The attitude kinematics in that paper are based on the quaternion, which must obey a normalization constraint that can be violated in the sigma-point filter since the predicted quaternion mean is derived using an averaged sum of quaternions. In this current paper an unconstrained three-component attitude-error vector is used to represent the quaternion error vector and the updates are performed using quaternion multiplication, leading to a natural way of maintaining the normalization constraint.[7] Also, Ref. 6 using an augmented matrix approach to handle process noise, which means that a decomposition of a matrix that has length equal to the length of the state vector plus the process-noise vector is required. In this paper a simple first-order trapezoidal approximation is used so that a decomposition of a matrix equal to the length of the state vector is only required. This significantly reduces the computational costs.

The organization of this paper proceeds as follows. First, the various coordinate frames used in INS are summarized. Conversions from the NED frame to the ECEF frame and vice versa are shown. Then, covariance mappings from the NED frame to the ECEF frame and vice versa are derived. Next, the linearized equations for the EKF using NED coordinates are shown, which are derived from a multiplicative quaternion approach. Then, a specific sigma-point filter, called the *Unscented filter*, is summarized followed by a review of the equations required to perform GPS/INS operations with this filter. Finally, simulation results are shown that compare the performance of the EKF with the Unscented filter with respect to initial condition errors.

II. Reference Frames

In this section the reference frames used to derive the GPS/INS equations are summarized, as shown in Figure 1:

- Earth-Centered-Inertial (ECI) Frame: denoted by $\{\hat{\mathbf{i}}_1, \hat{\mathbf{i}}_2, \hat{\mathbf{i}}_3\}$. The $\hat{\mathbf{i}}_1$ axis points toward the vernal equinox direction (also known as the "First Point of Aries" or the "vernal equinox point"), the $\hat{\mathbf{i}}_3$ axis points in the direction of the North pole and the $\hat{\mathbf{i}}_2$ axis completes the right-handed system (note that the $\hat{\mathbf{i}}_1$ and $\hat{\mathbf{i}}_2$ axes are on the equator, which is the fundamental plane). The ECI frame is non-rotating with respect to the stars (except for precession of equinoxes) and the Earth turns relative to this frame.[8] Vectors described using ECI coordinates will have a superscript I (e.g., $\mathbf{r}^I$).

- Earth-Centered-Earth-Fixed (ECEF) Frame: denoted by $\{\hat{\mathbf{e}}_1, \hat{\mathbf{e}}_2, \hat{\mathbf{e}}_3\}$. This frame is similar to the ECI frame with $\hat{\mathbf{e}}_3 = \hat{\mathbf{i}}_3$; however, the $\hat{\mathbf{e}}_1$ axis points in the direction of the Earth's prime meridian, and the $\hat{\mathbf{e}}_2$ axis completes the right-handed system. Unlike the ECI frame, the ECEF frame rotates with the Earth. The rotation angle is denoted by Θ in Figure 1. Vectors described using ECEF coordinates will have a superscript E (e.g., $\mathbf{r}^E$).

- North-East-Down (NED) Frame: denoted by $\{\hat{\mathbf{n}}, \hat{\mathbf{e}}, \hat{\mathbf{d}}\}$. This frame is used for local navigation purposes. It is formed by fitting a tangent plane to the geodetic reference ellipse at a point of interest.[3] The $\hat{\mathbf{n}}$ axis points true North, the $\hat{\mathbf{e}}$ points East, and the $\hat{\mathbf{d}}$ axis completes the right-handed system, which points in the direction of the interior of the Earth perpendicular to the reference ellipsoid. Vectors described using ECI coordinates will have a superscript N (e.g., $\mathbf{r}^N$).

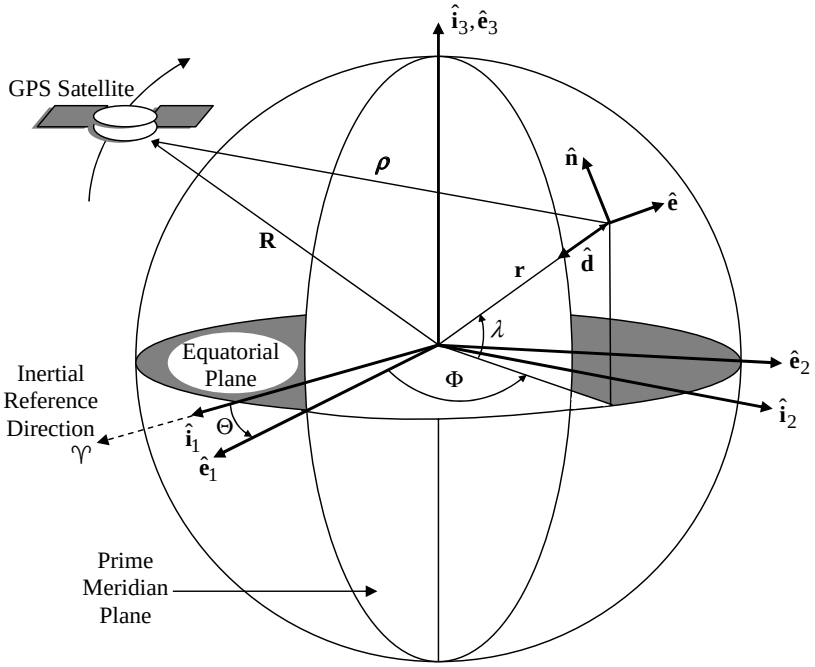

Figure 1. Definitions of Various Reference Frames

- Body Frame: denoted by $\{\hat{\mathbf{b}}_1, \hat{\mathbf{b}}_2, \hat{\mathbf{b}}_3\}$. This frame is fixed onto the vehicle body and rotates with it. Conventions typically depend on the particular vehicle. Vectors described using body-frame coordinates will have a superscript B (e.g., $\mathbf{r}^B$).

We now discuss the transformations between these reference frames. The transformation from the ECI frame to the ECEF frame follows

$$\begin{bmatrix} x \\ y \\ z \end{bmatrix}^E = \begin{bmatrix} \cos\Theta & \sin\Theta & 0 \\ -\sin\Theta & \cos\Theta & 0 \\ 0 & 0 & 1 \end{bmatrix} \begin{bmatrix} x \\ y \\ z \end{bmatrix}^I \tag{1}$$

where $\{x, y, z\}^I$ are the components of the ECI position vector, and $\{x, y, z\}^E$ are the components of the ECEF position vector. In order to determine the ECEF position vector we must first determine the angle Θ, which is related to time. A solar day is the length of time that elapses between the Sun reaching its highest point in the sky two consecutive times. However, the ECI coordinate system is fixed relative to the stars, not the Sun. A *sidereal day* is the length of time that passes between a given fixed star in the sky crossing a given projected meridian. A sidereal day is 4 minutes shorter than a solar day.[8] The Greenwich Mean Sidereal Time (GMST) is the mean sidereal time at zero longitude, which can be given by the angle Θ. Several formulas for the conversion from Universal Time (UT) to GMST are given in the open literature (e.g., see Ref. 9). One of the most widely-used formulas is presented by Meeus.[10]

The ECEF position vector is useful since this gives a simple approach to determine the longitude and latitude of a user. The Earth's geoid can be approximated by an ellipsoid of revolution about its minor axis. A common ellipsoid model is given by the World Geodetic System 1984 model (WGS-84), with semimajor axis $a = 6,378,137.0$ m and semiminor axis $b = 6,356,752.3142$ m. The eccentricity of this ellipsoid is given by $e = 0.0818$. The geodetic coordinates are given by the latitude λ, longitude Φ and height h. To determine the ECEF position vector, the length of the normal to the ellipsoid is first computed, given by[3]

$$N = \frac{a}{\sqrt{1 - e^2 \sin^2 \lambda}} \tag{2}$$

Then, given the observer geodetic quantities λ, Φ and h, the observer ECEF position coordinates are computed using

$$x = (N + h)\cos\lambda\cos\Phi \tag{3a}$$

$$y = (N + h)\cos\lambda\sin\Phi \tag{3b}$$

$$z = [N(1 - e^2) + h]\sin\lambda \tag{3c}$$

The conversion from ECEF to geodetic coordinates is not that straightforward. A complicated closed-form solution is given in Ref. 3, but a good approximation up to low Earth orbit is given by[11]

$$p = \sqrt{x^2 + y^2}, \quad \zeta = \text{atan}\left(\frac{z\,a}{p\,b}\right), \quad \bar{e}^2 = \frac{a^2 - b^2}{b^2} \tag{4a}$$

$$\lambda = \text{atan}\left(\frac{z + \bar{e}^2\,b\,\sin^3\zeta}{p - e^2\,a\,\cos^3\zeta}\right) \tag{4b}$$

$$\Phi = \text{atan2}(y,\, x) \tag{4c}$$

$$h = \frac{p}{\cos\lambda} - N \tag{4d}$$

where N is given by Eq. (2) and atan2 is a four quadrant inverse tangent function.

The conversion from ECEF coordinates to NED coordinates involves a rotation matrix from the known latitude and longitude. By the definition of the NED frame, a vehicle is fixed within this frame. This frame serves to define local directions for the velocity vector determined in a frame in which the vehicle has motion, such as the ECEF frame.[4] The velocity in NED coordinates is given by

$$\mathbf{v}^N \equiv \begin{bmatrix} v_N \\ v_E \\ v_D \end{bmatrix} = A_E^N \dot{\mathbf{r}}^E \tag{5}$$

where $\dot{\mathbf{r}}^E$ is the vehicle velocity in ECEF coordinates and A_E^N is the transformation matrix from the ECEF frame to the NED frame. We should note that $\mathbf{v}^N \neq \dot{\mathbf{r}}^N$ in general since $\dot{\mathbf{r}}^N = \mathbf{v}^N - \boldsymbol{\omega}_{N/E}^N \times \mathbf{r}^N$, where $\boldsymbol{\omega}_{N/E}^N$ is the angular velocity of the N frame relative to the E frame expressed in N coordinates. This relationship can be derived by differentiating $\mathbf{r}^N = A_E^N \mathbf{r}^E$. The NED frame is generally not used to provide a vehicle's positional coordinates, but rather to provide local directions along which the velocities may be indicated. The positions are determined by relating the velocity $\mathbf{v}^N$ with the derivatives of latitude, longitude and height, and integrating the resulting equations (see Ref. 4 for more details). The transformation matrix is given by[3]

$$A_E^N = \begin{bmatrix} -\sin\lambda\cos\Phi & -\sin\lambda\sin\Phi & \cos\lambda \\ -\sin\Phi & \cos\Phi & 0 \\ -\cos\lambda\cos\Phi & -\cos\lambda\sin\Phi & -\sin\lambda \end{bmatrix} \tag{6}$$

The attitude matrix which maps the NED frame to the vehicle body frame is given by

$$A_N^B = \begin{bmatrix} \cos\psi\cos\theta & \sin\psi\cos\theta & -\sin\theta \\ -\sin\psi\cos\phi + \cos\psi\sin\theta\sin\phi & \cos\psi\cos\phi + \sin\psi\sin\theta\sin\phi & \cos\theta\sin\phi \\ \sin\psi\sin\phi + \cos\psi\sin\theta\cos\phi & -\cos\psi\sin\phi + \sin\psi\sin\theta\cos\phi & \cos\theta\cos\phi \end{bmatrix} \tag{7}$$

where ϕ, θ and ψ are the roll, pitch and yaw angles, respectively. Note that the transformation from the ECEF to the body frame is simply given by $A_E^B = A_N^B A_E^N$.

A. Covariance Mappings

In this section various covariance mappings from the ECEF frame to the the NED frame and vice versa are shown. These expressions are required since the Kalman filter will be developed in ECEF coordinates. Denote the covariance associated with the attitude matrix that maps the ECEF frame to the body frame by $P_{\text{att}}^{\text{ECEF}}$. The covariance of the attitude matrix that maps the NED frame to the body frame, denoted by $P_{\text{att}}^{\text{NED}}$, is given by

$$P_{\text{att}}^{\text{NED}} = A_E^N P_{\text{att}}^{\text{ECEF}} A_N^E \tag{8}$$

where A_N^E is the transpose of A_E^N. The velocity covariance follows from Eq. (5):

$$P_{\text{vel}}^{\text{NED}} = A_E^N P_{\text{vel}}^{\text{ECEF}} A_N^E \tag{9}$$

The covariance of latitude, longitude and height from the ECEF position covariance is more difficult. To determine this quantity we require the partials of Eq. (4) with respect to x, y and z. The partials are given by

$$\frac{\partial \lambda}{\partial x} = \frac{1}{1+u^2}\frac{\partial u}{\partial x}, \quad \frac{\partial \lambda}{\partial y} = \frac{1}{1+u^2}\frac{\partial u}{\partial y}, \quad \frac{\partial \lambda}{\partial z} = \frac{1}{1+u^2}\frac{\partial u}{\partial z} \tag{10}$$

where u is defined by

$$u \equiv \frac{z + \bar{e}^2\, b\, \sin^3\zeta}{p - e^2\, a\, \cos^3\zeta} \tag{11}$$

The partials of u with respect to x, y and z are given by

$$\begin{aligned}\frac{\partial u}{\partial x} =& -\frac{(z + \bar{e}^2\, b\, \sin^3\zeta)}{(p - e^2\, a\, \cos^3\zeta)^2}\left(\frac{x}{p} + e^2\, a\, \frac{\partial \zeta}{\partial x}\sin\zeta\, \cos^2\zeta\right) \\ &+ \frac{3\bar{e}^2 b\, \sin^2\zeta\, \cos\zeta}{p - e^2\, a\, \cos^3\zeta}\frac{\partial \zeta}{\partial x}\end{aligned} \tag{12a}$$

$$\begin{aligned}\frac{\partial u}{\partial x} =& -\frac{(z + \bar{e}^2\, b\, \sin^3\zeta)}{(p - e^2\, a\, \cos^3\zeta)^2}\left(\frac{y}{p} + e^2\, a\, \frac{\partial \zeta}{\partial y}\sin\zeta\, \cos^2\zeta\right) \\ &+ \frac{3\bar{e}^2 b\, \sin^2\zeta\, \cos\zeta}{p - e^2\, a\, \cos^3\zeta}\frac{\partial \zeta}{\partial y}\end{aligned} \tag{12b}$$

$$\begin{aligned}\frac{\partial u}{\partial x} =& \left[\frac{3\bar{e}^2 b\, \sin^2\zeta\, \cos\zeta}{p - e^2\, a\, \cos^3\zeta} - \frac{(z + \bar{e}^2\, b\, \sin^3\zeta)(e^2\, a\, \sin\zeta\, \cos^2\zeta)}{(p - e^2\, a\, \cos^3\zeta)^2}\right]\frac{\partial \zeta}{\partial z} \\ &+ \frac{1}{p - e^2\, a\, \cos^3\zeta}\end{aligned} \tag{12c}$$

where

$$\frac{\partial \zeta}{\partial x} = -\frac{x\, z\, a\, b}{p\,(p^2\, b^2 + z^2\, a^2)}, \quad \frac{\partial \zeta}{\partial y} = -\frac{y\, z\, a\, b}{p\,(p^2\, b^2 + z^2\, a^2)}, \quad \frac{\partial \zeta}{\partial z} = \frac{p\, a\, b}{p^2\, b^2 + z^2\, a^2} \tag{13}$$

The partials of Eq. (4c) with respect to x, y and z are given by

$$\frac{\partial \Phi}{\partial x} = -\frac{y}{x^2 + y^2}, \quad \frac{\partial \Phi}{\partial y} = \frac{x}{x^2 + y^2}, \quad \frac{\partial \Phi}{\partial z} = 0 \tag{14}$$

The partials of Eq. (4d) with respect to x, y and z are given by

$$\frac{\partial h}{\partial x} = \frac{x}{p\, \cos\lambda} + \left(\frac{p\, \sin\lambda}{\cos^2\lambda} - \frac{\partial N}{\partial \lambda}\right)\frac{\partial \lambda}{\partial x} \tag{15a}$$

$$\frac{\partial h}{\partial y} = \frac{y}{p\, \cos\lambda} + \left(\frac{p\, \sin\lambda}{\cos^2\lambda} - \frac{\partial N}{\partial \lambda}\right)\frac{\partial \lambda}{\partial y} \tag{15b}$$

$$\frac{\partial h}{\partial z} = \left(\frac{p\, \sin\lambda}{\cos^2\lambda} - \frac{\partial N}{\partial \lambda}\right)\frac{\partial \lambda}{\partial z} \tag{15c}$$

where

$$\frac{\partial N}{\partial \lambda} = \frac{a\, e^2 \sin\lambda \cos\lambda}{(1 - e^2 \sin^2\lambda)^{3/2}} \tag{16}$$

Next, the following sensitivity matrix is formed:

$$H \equiv \begin{bmatrix} \dfrac{\partial \lambda}{\partial x} & \dfrac{\partial \lambda}{\partial y} & \dfrac{\partial \lambda}{\partial z} \\ \dfrac{\partial \Phi}{\partial x} & \dfrac{\partial \Phi}{\partial y} & \dfrac{\partial \Phi}{\partial z} \\ \dfrac{\partial h}{\partial x} & \dfrac{\partial h}{\partial y} & \dfrac{\partial h}{\partial z} \end{bmatrix} \tag{17}$$

Then, the covariance of the latitude, longitude and height, denoted by $P_{\text{pos}}^{\text{LLH}}$, is given by

$$P_{\text{pos}}^{\text{LLH}} = H\, P_{\text{pos}}^{\text{ECEF}} H^T \tag{18}$$

where $P_{\text{pos}}^{\text{ECEF}}$ denotes the covariance of the ECEF position errors.

The attitude and velocity mappings from the NED frame to the ECEF frame is straightforward from Eqs. (8) and (9), each given by $P_{\text{att}}^{\text{ECEF}} = A_N^E P_{\text{att}}^{\text{NED}} A_E^N$ and $P_{\text{vel}}^{\text{ECEF}} = A_N^E P_{\text{vel}}^{\text{NED}} A_E^N$. The covariance of ECEF positions from the latitude, longitude and height covariance is derived by taking the partials of the quantities in Eq. (3) with respect to λ, Φ and h, which leads to the following partial matrix:

$$\mathcal{H} = \begin{bmatrix} \dfrac{\partial N}{\partial \lambda}\cos\lambda\cos\Phi - (N+h)\sin\lambda\cos\Phi & -(N+h)\cos\lambda\sin\Phi & \cos\lambda\cos\Phi \\ \dfrac{\partial N}{\partial \lambda}\cos\lambda\sin\Phi - (N+h)\sin\lambda\sin\Phi & (N+h)\cos\lambda\cos\Phi & \cos\lambda\sin\Phi \\ \dfrac{\partial N}{\partial \lambda}(1-e^2)\sin\lambda + [N(1-e^2)+h]\cos\lambda & 0 & \sin\lambda \end{bmatrix} \tag{19}$$

Then, the covariance of the ECEF position covariance is given by

$$P_{\text{pos}}^{\text{ECEF}} = \mathcal{H}\, P_{\text{pos}}^{\text{LLH}} \mathcal{H}^T \tag{20}$$

III. Attitude Kinematics

In this section the basic properties of attitude kinematics are summarized. The attitude matrix involves a total of nine parameters, but they are clearly not independent. Various parameterizations of the attitude matrix can be used: Euler angles, Euler axis and rotation angle, quaternions, Rodrigues parameters, etc.[12] One of the most useful attitude parameterization is given by the quaternion,[13] which is a four-dimensional vector, defined as $\mathbf{q} \equiv [\boldsymbol{\varrho}^T \;\; q_4]^T$, with $\boldsymbol{\varrho} \equiv [q_1 \;\; q_2 \;\; q_3]^T = \hat{\mathbf{e}}\sin(\vartheta/2)$ and $q_4 = \cos(\vartheta/2)$, where $\hat{\mathbf{e}}$ is the axis of rotation and ϑ is the angle of rotation. Since a four-dimensional vector is used to describe three dimensions, the quaternion components cannot be independent of each other. The quaternion satisfies a single constraint given by $\mathbf{q}^T\mathbf{q} = 1$, which is analogous to requiring that $\hat{\mathbf{e}}$ be a unit vector in the Euler axis/angle parameterization.[12] The attitude matrix that transform the NED frame to the body frame is related to the quaternion by

$$A_N^B(\mathbf{q}) = \Xi^T(\mathbf{q})\Psi(\mathbf{q}) \tag{21}$$

with

$$\Xi(\mathbf{q}) \equiv \begin{bmatrix} q_4 I_{3\times 3} + [\boldsymbol{\varrho}\times] \\ -\boldsymbol{\varrho}^T \end{bmatrix}, \quad \Psi(\mathbf{q}) \equiv \begin{bmatrix} q_4 I_{3\times 3} - [\boldsymbol{\varrho}\times] \\ -\boldsymbol{\varrho}^T \end{bmatrix} \tag{22}$$

where $[\boldsymbol{\varrho}\times]$ is the cross product matrix, defined by

$$[\boldsymbol{\varrho}\times] \equiv \begin{bmatrix} 0 & -q_3 & q_2 \\ q_3 & 0 & q_1 \\ -q_2 & q_1 & 0 \end{bmatrix} \tag{23}$$

An advantage to using quaternions is that the attitude matrix is quadratic in the parameters and also does not involve transcendental functions. For small angles the vector part of the quaternion is approximately equal to half angles so that $\boldsymbol{\varrho} \approx \boldsymbol{\alpha}/2$ and $q_4 \approx 1$, where $\boldsymbol{\alpha}$ is a vector of the roll, pitch and yaw angles. The attitude matrix can then be approximated by $A_N^B \approx I_{3\times 3} - [\boldsymbol{\alpha}\times]$ which is valid to within first-order in the angles.

The attitude kinematics equation is given by

$$\dot{A}_N^B = -[\boldsymbol{\omega}_{B/N}^B\times]A_N^B \tag{24}$$

where $\boldsymbol{\omega}_{B/N}^B$ is angular velocity of the B frame relative to the N frame expressed in B coordinates. Another form of Eq. (24) is given by

$$\dot{A}_B^N = A_B^N[\boldsymbol{\omega}_{B/N}^B\times] \tag{25}$$

which will be used in the derivation of the INS equations. The quaternion kinematics equation is given by

$$\dot{\mathbf{q}} = \frac{1}{2}\Xi(\mathbf{q})\boldsymbol{\omega}^B_{B/N} = \frac{1}{2}\Omega(\boldsymbol{\omega}^B_{B/N})\mathbf{q} \tag{26}$$

where

$$\Omega(\boldsymbol{\omega}^B_{B/N}) \equiv \begin{bmatrix} -[\boldsymbol{\omega}^B_{B/N}\times] & \boldsymbol{\omega}^B_{B/N} \\ -(\boldsymbol{\omega}^B_{B/N})^T & 0 \end{bmatrix} \tag{27}$$

A major advantage of using quaternions is that the kinematics equation is linear in the quaternion and is also free of singularities. Another advantage of quaternions is that successive rotations can be accomplished using quaternion multiplication. Here we adopt the convention of Lefferts, Markley, and Shuster[14] who multiply the quaternions in the same order as the attitude matrix multiplication (in contrast to the usual convention established by Hamiliton[13]). Suppose we wish to perform a successive rotation. This can be written using

$$A(\mathbf{q}')A(\mathbf{q}) = A(\mathbf{q}' \otimes \mathbf{q}) \tag{28}$$

The composition of the quaternions is bilinear, with

$$\mathbf{q}' \otimes \mathbf{q} = \begin{bmatrix} \Psi(\mathbf{q}') & \mathbf{q}' \end{bmatrix} \mathbf{q} = \begin{bmatrix} \Xi(\mathbf{q}) & \mathbf{q} \end{bmatrix} \mathbf{q}' \tag{29}$$

Also, the inverse quaternion is defined by

$$\mathbf{q}^{-1} \equiv \begin{bmatrix} -\boldsymbol{\varrho} \\ q_4 \end{bmatrix} \tag{30}$$

Note that $\mathbf{q} \otimes \mathbf{q}^{-1} = [0\ 0\ 0\ 1]^T$, which is the identity quaternion. A computationally efficient algorithm to extract the quaternion from the attitude matrix is given in Ref. 15. A more thorough review of the attitude representations shown in this section, as well as others, can be found in the excellent survey paper by Shuster[12] and in the book by Kuipers.[16]

IV. INS Basic Equations

The basic INS equations using NED coordinates with the quaternion parameterization are given by[3,4]

$$\dot{\mathbf{q}} = \frac{1}{2}\Xi(\mathbf{q})\boldsymbol{\omega}^B_{B/N} \tag{31a}$$

$$\dot{\lambda} = \frac{v_N}{R_\lambda + h} \tag{31b}$$

$$\dot{\Phi} = \frac{v_E}{(R_\Phi + h)\cos\lambda} \tag{31c}$$

$$\dot{h} = -v_D \tag{31d}$$

$$\dot{v}_N = -\left[\frac{v_E}{(R_\Phi + h)\cos\lambda} + 2\omega_e\right] v_E \sin\lambda + \frac{v_N v_D}{R_\lambda + h} + a_N \tag{31e}$$

$$\dot{v}_E = \left[\frac{v_E}{(R_\Phi + h)\cos\lambda} + 2\omega_e\right] v_N \sin\lambda + \frac{v_E v_D}{R_\Phi + h} + 2\omega_e v_D \cos\lambda + a_E \tag{31f}$$

$$\dot{v}_D = -\frac{v_E^2}{R_\Phi + h} - \frac{v_N^2}{R_\lambda + h} - 2\omega_e v_E \cos\lambda + g + a_D \tag{31g}$$

where ω_e is the Earth's rotation rate given as (from WGS-84) 7.292115×10^{-5} rad/sec, and

$$R_\lambda = \frac{a(1-e^2)}{(1 - e^2\sin^2\lambda)^{3/2}} \tag{32a}$$

$$R_\Phi = \frac{a}{(1 - e^2\sin^2\lambda)^{1/2}} \tag{32b}$$

The local gravity, g, using WGS-84 parameters is given by

$$\begin{aligned} g = {} & 9.780327(1 + 5.3024 \times 10^{-3} \sin^2 \lambda - 5.8 \times 10^{-6} \sin^2 2\lambda) \\ & - (3.0877 \times 10^{-6} - 4.4 \times 10^{-9} \sin^2 \lambda)h + 7.2 \times 10^{-14} h^2 \ \ \mathrm{m/s^2} \end{aligned} \tag{33}$$

where h is measured in meters. Note that Eq. (31a) cannot be used directly with the gyro measurement. However, this problem can be overcome by using the following identity:

$$\boldsymbol{\omega}^B_{B/I} = \boldsymbol{\omega}^B_{B/N} + \boldsymbol{\omega}^B_{N/I} \tag{34}$$

Solving Eq. (34) for $\boldsymbol{\omega}^B_{B/N}$ and substituting $\boldsymbol{\omega}^B_{N/I} = A^B_N(\mathbf{q})\boldsymbol{\omega}^N_{N/I}$ yields

$$\boldsymbol{\omega}^B_{B/N} = \boldsymbol{\omega}^B_{B/I} - A^B_N(\mathbf{q})\boldsymbol{\omega}^N_{N/I} \tag{35}$$

where

$$\boldsymbol{\omega}^N_{N/I} = w_e \begin{bmatrix} \cos\lambda \\ 0 \\ -\sin\lambda \end{bmatrix} + \begin{bmatrix} \dfrac{v_E}{R_\Phi + h} \\ -\dfrac{v_N}{R_\lambda + h} \\ -\dfrac{v_E \tan\lambda}{R_\Phi + h} \end{bmatrix} \tag{36}$$

Now Eq. (31a) can be related to the gyro measurements. Also, the acceleration variables are related to the accelerometer measurements through

$$\mathbf{a}^N \equiv \begin{bmatrix} a_N \\ a_E \\ a_D \end{bmatrix} = A^N_B(\mathbf{q})\mathbf{a}^B \tag{37}$$

where $\mathbf{a}^B$ is the acceleration vector in body coordinates and $A^N_B(\mathbf{q})$ is the matrix transpose of $A^B_N(\mathbf{q})$.

The gyro measurement model is given by

$$\tilde{\boldsymbol{\omega}}^B_{B/I} = (I_{3\times3} + \mathcal{K}_g)\boldsymbol{\omega}^B_{B/I} + \mathbf{b}_g + \boldsymbol{\eta}_{gv} \tag{38a}$$

$$\dot{\mathbf{b}}_g = \boldsymbol{\eta}_{gu} \tag{38b}$$

where $\mathbf{b}_g$ is the gyro "bias", $\mathcal{K}_g$ is a diagonal matrix of gyro scale factors, and $\boldsymbol{\eta}_{gv}$ and $\boldsymbol{\eta}_{gu}$ are zero-mean Gaussian white-noise processes with spectral densities given by $\sigma^2_{gv} I_{3\times3}$ and $\sigma^2_{gu} I_{3\times3}$, respectively. The accelerometer measurement model is given by

$$\tilde{\mathbf{a}}^B = (I_{3\times3} + \mathcal{K}_g)\mathbf{a}^B + \mathbf{b}_a + \boldsymbol{\eta}_{av} \tag{39a}$$

$$\dot{\mathbf{b}}_a = \boldsymbol{\eta}_{au} \tag{39b}$$

where $\mathbf{b}_a$ is the accelerometer "bias", $\mathcal{K}_a$ is a diagonal matrix of accelerometer scale factors, and $\boldsymbol{\eta}_{av}$ and $\boldsymbol{\eta}_{au}$ are zero-mean Gaussian white-noise processes with spectral densities given by $\sigma^2_{av} I_{3\times3}$ and $\sigma^2_{au} I_{3\times3}$, respectively. We should note that most manufacturers give values for σ_{gv} and σ_{av}, but not σ_{gu} and σ_{au}. The scale factors are assumed to be small enough so that the approximation $(I + \mathcal{K})^{-1} \approx (I - \mathcal{K})$ is valid for both the gyros and acclerometers. Simulating gyro and accelerometer using computers is not easy since continuous measurements cannot be generated using digital computers. A discrete-time simulation is possible using the spectral densities though, which is shown in the Appendix. The same model can be used for the accelerometer measurements.

V. Extended Kalman Filter Equations

In this section the implementation equations for the EKF are shown. The estimated quantities are given by

$$\dot{\hat{\mathbf{q}}} = \frac{1}{2}\Xi(\hat{\mathbf{q}})\hat{\boldsymbol{\omega}}^B_{B/N} \tag{40a}$$

$$\hat{\boldsymbol{\omega}}^B_{B/N} = (I_{3\times 3} - \hat{\mathcal{K}}_g)(\tilde{\boldsymbol{\omega}}^B_{B/I} - \hat{\mathbf{b}}_g) - A^B_N(\hat{\mathbf{q}})\hat{\boldsymbol{\omega}}^N_{N/I} \tag{40b}$$

$$\dot{\hat{\lambda}} = \frac{\hat{v}_N}{\hat{R}_\lambda + \hat{h}} \tag{40c}$$

$$\dot{\hat{\Phi}} = \frac{\hat{v}_E}{(\hat{R}_\Phi + \hat{h})\cos\hat{\lambda}} \tag{40d}$$

$$\dot{\hat{h}} = -\hat{v}_D \tag{40e}$$

$$\dot{\hat{v}}_N = -\left[\frac{\hat{v}_E}{(\hat{R}_\Phi + \hat{h})\cos\hat{\lambda}} + 2\omega_e\right]\hat{v}_E \sin\hat{\lambda} + \frac{\hat{v}_N\hat{v}_D}{\hat{R}_\lambda + \hat{h}} + \hat{a}_N \tag{40f}$$

$$\dot{\hat{v}}_E = \left[\frac{\hat{v}_E}{(\hat{R}_\Phi + \hat{h})\cos\hat{\lambda}} + 2\omega_e\right]\hat{v}_N \sin\hat{\lambda} + \frac{\hat{v}_E\hat{v}_D}{\hat{R}_\Phi + \hat{h}} + 2\omega_e\hat{v}_D\cos\hat{\lambda} + \hat{a}_E \tag{40g}$$

$$\dot{\hat{v}}_D = -\frac{\hat{v}^2_E}{\hat{R}_\Phi + \hat{h}} - \frac{\hat{v}^2_N}{\hat{R}_\lambda + \hat{h}} - 2\omega_e\hat{v}_E\cos\hat{\lambda} + \hat{g} + \hat{a}_D \tag{40h}$$

$$\hat{\mathbf{a}}^N \equiv \begin{bmatrix}\hat{a}_N \\ \hat{a}_E \\ \hat{a}_D\end{bmatrix} = A^N_B(\hat{\mathbf{q}})\hat{\mathbf{a}}^B \tag{40i}$$

$$\hat{\mathbf{a}}^B = (I_{3\times 3} - \hat{\mathcal{K}}_a)(\tilde{\mathbf{a}}^B - \hat{\mathbf{b}}_a) \tag{40j}$$

$$\dot{\hat{\mathbf{b}}}_g = \mathbf{0} \tag{40k}$$

$$\dot{\hat{\mathbf{b}}}_a = \mathbf{0} \tag{40l}$$

$$\dot{\hat{\mathbf{k}}}_g = \mathbf{0} \tag{40m}$$

$$\dot{\hat{\mathbf{k}}}_a = \mathbf{0} \tag{40n}$$

where $\hat{\mathbf{k}}_g$ and $\hat{\mathbf{k}}_a$ are the elements of the diagonal matrices $\hat{\mathcal{K}}_g$ and $\hat{\mathcal{K}}_a$, respectively. Also, $\hat{\boldsymbol{\omega}}^N_{N/I}$, $\hat{R}_\lambda$, $\hat{R}_\Phi$ and $\hat{g}$ are evaluated at the current estimates. Note that the attitude matrix is coupled into the position now, which allows us to estimate the attitude from position measurements.

We now derive the error equations, which are used in the EKF covariance propagation. The quaternion is linearized using a multiplicative approach.[14] First, an error quaternion is defined by

$$\boldsymbol{\delta}\mathbf{q} = \mathbf{q} \otimes \hat{\mathbf{q}}^{-1} \tag{41}$$

with $\boldsymbol{\delta}\mathbf{q} \equiv [\boldsymbol{\delta\varrho}^T \;\; \delta q_4]^T$, where the quaternion multiplication is defined by Eq. (29). The equivalent attitude error matrix is given by

$$A^B_N(\boldsymbol{\delta}\mathbf{q}) = A^B_N(\mathbf{q})\left[A^B_N(\hat{\mathbf{q}})\right]^T \tag{42}$$

If the error quaternion is "small" then to within first order we have $\boldsymbol{\delta\varrho} \approx \boldsymbol{\delta\alpha}/2$ and $\delta q_4 \approx 1$, where $\boldsymbol{\delta\alpha}$ is a small error-angle rotation vector. Also, the quaternion inverse is defined by Eq. (30). The linearized model error-kinematics follow[17]

$$\dot{\boldsymbol{\delta\alpha}} = -[\hat{\boldsymbol{\omega}}^B_{B/N}\times]\boldsymbol{\delta\alpha} + \boldsymbol{\delta\omega}^B_{B/I} - A(\hat{\mathbf{q}})\boldsymbol{\delta\omega}^N_{N/I} \tag{43a}$$

$$\delta\dot{q}_4 = 0 \tag{43b}$$

where $\boldsymbol{\delta\omega}^B_{B/I} = \boldsymbol{\omega}^B_{B/I} - \hat{\boldsymbol{\omega}}^B_{B/I}$ and $\boldsymbol{\delta\omega}^N_{N/I} = \boldsymbol{\omega}^N_{N/I} - \hat{\boldsymbol{\omega}}^N_{N/I}$. Note that the fourth error-quaternion component is constant. The first-order approximation, which assumes that the true quaternion is "close" to the estimated quaternion, gives $\delta q_4 \approx 1$. This allows us to reduce the order of the system in the EKF by one state.

The linearization using Eq. (41) maintains quaternion normalization to within first-order if the estimated quaternion is "close" to the true quaternion, which is within the first-order approximation in the EKF. The error $\boldsymbol{\delta\omega}^B_{B/I}$ to within first-order can be written as

$$\boldsymbol{\delta\omega}^B_{B/I} = -\left[(I_{3\times3} - \hat{\mathcal{K}}_g)\Delta\mathbf{b}_g + (\tilde{\Omega}^B_{B/I} - \hat{B}_g)\Delta\mathbf{k}_g + (I_{3\times3} - \hat{\mathcal{K}}_g)\boldsymbol{\eta}_{gv}\right] \tag{44}$$

where $\Delta\mathbf{b}_g = \mathbf{b}_g - \hat{\mathbf{b}}_g$, $\Delta\mathbf{k}_g = \mathbf{k}_g - \hat{\mathbf{k}}_g$, $\tilde{\Omega}^B_{B/I}$ is a diagonal matrix of the elements of $\tilde{\boldsymbol{\omega}}^B_{B/I}$ and $\hat{B}_g$ is a diagonal matrix of the elements of $\hat{\mathbf{b}}_g$. The error $\boldsymbol{\delta\omega}^N_{N/I}$ can be computed using a first-order Taylor series expansion. This yields

$$\begin{aligned}\boldsymbol{\delta\dot{\alpha}} = &-\left[(I_{3\times3} - \hat{\mathcal{K}}_g)(\tilde{\boldsymbol{\omega}}^B_{B/I} - \hat{\mathbf{b}}_g)\times\right]\boldsymbol{\delta\alpha} - (I_{3\times3} - \hat{\mathcal{K}}_g)\Delta\mathbf{b}_g - (\tilde{\Omega}^B_{B/I} - \hat{B}_g)\Delta\mathbf{k}_g - (I_{3\times3} - \hat{\mathcal{K}}_g)\boldsymbol{\eta}_{gv} \\ &- A^B_N(\mathbf{q})\left.\frac{\partial\boldsymbol{\omega}^N_{N/I}}{\partial\mathbf{p}}\right|_{\hat{\mathbf{p}},\hat{\mathbf{v}}^N}\Delta\mathbf{p} - A^B_N(\mathbf{q})\left.\frac{\partial\boldsymbol{\omega}^N_{N/I}}{\partial\mathbf{v}^N}\right|_{\hat{\mathbf{p}}}\Delta\mathbf{v}^N\end{aligned} \tag{45}$$

where $\mathbf{p} \equiv [\lambda \;\; \Phi \;\; h]^T$, $\Delta\mathbf{p} = \mathbf{p} - \hat{\mathbf{p}}$ and $\Delta\mathbf{v}^N = \mathbf{v}^N - \hat{\mathbf{v}}^N$. The partials are given by

$$\frac{\partial\boldsymbol{\omega}^N_{N/I}}{\partial\mathbf{p}} = \begin{bmatrix} -\omega_e\sin\lambda - \dfrac{v_E}{(R_\Phi+h)^2}\dfrac{\partial R_\Phi}{\partial\lambda} & 0 & -\dfrac{v_E}{(R_\Phi+h)^2} \\ \dfrac{v_N}{(R_\lambda+h)^2}\dfrac{\partial R_\lambda}{\partial\lambda} & 0 & \dfrac{v_N}{(R_\lambda+h)^2} \\ -\omega_e\cos\lambda - \dfrac{v_E\sec^2\lambda}{R_\Phi+h} + \dfrac{v_E\tan\lambda}{(R_\Phi+h)^2}\dfrac{\partial R_\Phi}{\partial\lambda} & 0 & \dfrac{v_E\tan\lambda}{(R_\Phi+h)^2} \end{bmatrix} \tag{46a}$$

$$\frac{\partial\boldsymbol{\omega}^N_{N/I}}{\partial\mathbf{v}^N} = \begin{bmatrix} 0 & \dfrac{1}{R_\Phi+h} & 0 \\ -\dfrac{1}{R_\lambda+h} & 0 & 0 \\ 0 & -\dfrac{\tan\lambda}{R_\Phi+h} & 0 \end{bmatrix} \tag{46b}$$

with

$$\frac{\partial R_\Phi}{\partial\lambda} = \frac{a\,e^2\sin\lambda\cos\lambda}{(1-e^2\sin^2\lambda)^{3/2}} \tag{47a}$$

$$\frac{\partial R_\lambda}{\partial\lambda} = \frac{3a(1-e^2)e^2\sin\lambda\cos\lambda}{(1-e^2\sin^2\lambda)^{5/2}} \tag{47b}$$

The error equations for the remaining states can be derived using a similar approach to derive the attitude-error equation.

The state, state-error vector, process noise vector and covariance used in the EKF are defined as

$$\mathbf{x} \equiv \begin{bmatrix}\mathbf{q}\\ \mathbf{p}\\ \mathbf{v}^N\\ \mathbf{b}_g\\ \mathbf{b}_a\\ \mathbf{k}_g\\ \mathbf{k}_a\end{bmatrix}, \quad \Delta\mathbf{x} \equiv \begin{bmatrix}\boldsymbol{\delta\alpha}\\ \Delta\mathbf{p}\\ \Delta\mathbf{v}^N\\ \Delta\mathbf{b}_g\\ \Delta\mathbf{b}_a\\ \Delta\mathbf{k}_g\\ \Delta\mathbf{k}_a\end{bmatrix}, \quad \mathbf{w} \equiv \begin{bmatrix}\boldsymbol{\eta}_{gv}\\ \boldsymbol{\eta}_{gu}\\ \boldsymbol{\eta}_{av}\\ \boldsymbol{\eta}_{au}\end{bmatrix} \tag{48a}$$

$$Q = \begin{bmatrix}\sigma^2_{gv}I_{3\times3} & 0_{3\times3} & 0_{3\times3} & 0_{3\times3}\\ 0_{3\times3} & \sigma^2_{gu}I_{3\times3} & 0_{3\times3} & 0_{3\times3}\\ 0_{3\times3} & 0_{3\times3} & \sigma^2_{av}I_{3\times3} & 0_{3\times3}\\ 0_{3\times3} & 0_{3\times3} & 0_{3\times3} & \sigma^2_{au}I_{3\times3}\end{bmatrix} \tag{48b}$$

The error-dynamics used in the EKF propagation are given by

$$\Delta\dot{\mathbf{x}} = F\Delta\mathbf{x} + G\mathbf{w} \tag{49}$$

where

$$F \equiv \begin{bmatrix} F_{11} & F_{12} & F_{13} & F_{14} & 0_{3\times3} & F_{16} & 0_{3\times3} \\ 0_{3\times3} & F_{22} & F_{23} & 0_{3\times3} & 0_{3\times3} & 0_{3\times3} & 0_{3\times3} \\ F_{31} & F_{32} & F_{33} & 0_{3\times3} & F_{35} & 0_{3\times3} & F_{37} \\ 0_{3\times3} & 0_{3\times3} & 0_{3\times3} & 0_{3\times3} & 0_{3\times3} & 0_{3\times3} & 0_{3\times3} \\ 0_{3\times3} & 0_{3\times3} & 0_{3\times3} & 0_{3\times3} & 0_{3\times3} & 0_{3\times3} & 0_{3\times3} \\ 0_{3\times3} & 0_{3\times3} & 0_{3\times3} & 0_{3\times3} & 0_{3\times3} & 0_{3\times3} & 0_{3\times3} \\ 0_{3\times3} & 0_{3\times3} & 0_{3\times3} & 0_{3\times3} & 0_{3\times3} & 0_{3\times3} & 0_{3\times3} \end{bmatrix} \tag{50a}$$

$$G \equiv \begin{bmatrix} -(I_{3\times3} - \hat{\mathcal{K}}_g) & 0_{3\times3} & 0_{3\times3} & 0_{3\times3} \\ 0_{3\times3} & 0_{3\times3} & 0_{3\times3} & 0_{3\times3} \\ 0_{3\times3} & 0_{3\times3} & -A_B^N(\hat{\mathbf{q}})(I_{3\times3} - \hat{\mathcal{K}}_a) & 0_{3\times3} \\ 0_{3\times3} & I_{3\times3} & 0_{3\times3} & 0_{3\times3} \\ 0_{3\times3} & 0_{3\times3} & 0_{3\times3} & I_{3\times3} \\ 0_{3\times3} & 0_{3\times3} & 0_{3\times3} & 0_{3\times3} \\ 0_{3\times3} & 0_{3\times3} & 0_{3\times3} & 0_{3\times3} \end{bmatrix} \tag{50b}$$

with

$$F_{11} = -\left[(I_{3\times3} - \hat{\mathcal{K}}_g)(\tilde{\boldsymbol{\omega}}_{B/I}^B - \hat{\mathbf{b}}_g)\times\right], \quad F_{12} = -A_N^B(\hat{\mathbf{q}})\left.\frac{\partial\boldsymbol{\omega}_{N/I}^N}{\partial\mathbf{p}}\right|_{\hat{\mathbf{p}},\hat{\mathbf{v}}^N}, \quad F_{13} = -A_N^B(\mathbf{q})\left.\frac{\partial\boldsymbol{\omega}_{N/I}^N}{\partial\mathbf{v}^N}\right|_{\hat{\mathbf{p}}} \tag{51a}$$

$$F_{14} = -(I_{3\times3} - \hat{\mathcal{K}}_g), \quad F_{16} = -(\tilde{\Omega}_{B/I}^B - \hat{B}_g) \tag{51b}$$

$$F_{22} = \left.\frac{\partial\dot{\mathbf{p}}}{\partial\mathbf{p}}\right|_{\hat{\mathbf{p}},\hat{\mathbf{v}}^N}, \quad F_{23} = \left.\frac{\partial\dot{\mathbf{p}}}{\partial\mathbf{v}^N}\right|_{\hat{\mathbf{p}}} \tag{51c}$$

$$F_{31} = -A_B^N(\hat{\mathbf{q}})[\hat{\mathbf{a}}^B\times], \quad F_{32} = \left.\frac{\partial\dot{\mathbf{v}}^N}{\partial\mathbf{p}}\right|_{\hat{\mathbf{p}},\hat{\mathbf{v}}^N}, \quad F_{33} = \left.\frac{\partial\dot{\mathbf{v}}^N}{\partial\mathbf{v}^N}\right|_{\hat{\mathbf{p}},\hat{\mathbf{v}}^N} \tag{51d}$$

$$F_{35} = -A_B^N(\hat{\mathbf{q}})(I_{3\times3} - \hat{\mathcal{K}}_a), \quad F_{37} = -A_B^N(\hat{\mathbf{q}})(\tilde{\mathcal{A}}^B - \hat{B}_a) \tag{51e}$$

where $\tilde{\mathcal{A}}^B$ is a diagonal matrix of the elements of $\tilde{\mathbf{a}}^B$ and $\hat{B}_a$ is a diagonal matrix of the elements of $\hat{\mathbf{b}}_a$. The position partials are given by

$$\frac{\partial\dot{\mathbf{p}}}{\partial\mathbf{p}} = \begin{bmatrix} -\dfrac{v_N}{(R_\lambda+h)^2}\dfrac{\partial R_\lambda}{\partial\lambda} & 0 & -\dfrac{v_N}{(R_\lambda+h)^2} \\ -\dfrac{v_E\sec\lambda}{(R_\Phi+h)^2}\dfrac{\partial R_\Phi}{\partial\lambda} + \dfrac{v_E\sec\lambda\tan\lambda}{R_\Phi+h} & 0 & -\dfrac{v_E\sec\lambda}{(R_\Phi+h)^2} \\ 0 & 0 & 0 \end{bmatrix}, \quad \frac{\partial\dot{\mathbf{p}}}{\partial\mathbf{v}^N} = \begin{bmatrix} \dfrac{1}{R_\lambda+h} & 0 & 0 \\ 0 & \dfrac{\sec\lambda}{R_\Phi+h} & 0 \\ 0 & 0 & -1 \end{bmatrix} \tag{52}$$

The velocity partials are given by

$$\frac{\partial\dot{\mathbf{v}}^N}{\partial\mathbf{p}} = \begin{bmatrix} Y_{11} & 0 & Y_{13} \\ Y_{21} & 0 & Y_{23} \\ Y_{31} & 0 & Y_{33} \end{bmatrix}, \quad \frac{\partial\dot{\mathbf{v}}^N}{\partial\mathbf{v}^N} = \begin{bmatrix} Z_{11} & Z_{12} & Z_{13} \\ Z_{21} & Z_{22} & Z_{23} \\ Z_{31} & Z_{32} & 0 \end{bmatrix} \tag{53}$$

where

$$Y_{11} = -\frac{v_E^2 \sec^2\lambda}{R_\Phi + h} + \frac{v_E^2 \tan\lambda}{(R_\Phi + h)^2}\frac{\partial R_\Phi}{\partial \lambda} - 2\omega_e v_E \cos\lambda - \frac{v_N v_D}{(R_\lambda + h)^2}\frac{\partial R_\lambda}{\partial \lambda} \tag{54a}$$

$$Y_{13} = \frac{v_E^2 \tan\lambda}{(R_\Phi + h)^2} - \frac{v_N v_D}{(R_\lambda + h)^2} \tag{54b}$$

$$Y_{21} = \frac{v_E\, v_N \sec^2\lambda}{R_\Phi + h} - \frac{v_E\, v_N \tan\lambda}{(R_\Phi + h)^2}\frac{\partial R_\Phi}{\partial \lambda} + 2\omega_e v_N \cos\lambda - \frac{v_E\, v_D}{(R_\Phi + h)^2}\frac{\partial R_\Phi}{\partial \lambda} - 2\omega_e v_D \sin\lambda \tag{54c}$$

$$Y_{23} = -v_E\left[\frac{v_N \tan\lambda + v_D}{(R_\Phi + h)^2}\right] \tag{54d}$$

$$Y_{31} = \frac{v_E^2}{(R_\Phi + h)^2}\frac{\partial R_\Phi}{\partial \lambda} + \frac{v_N^2}{(R_\lambda + h)^2}\frac{\partial R_\lambda}{\partial \lambda} + 2\omega_e v_E \sin\lambda + \frac{\partial g}{\partial \lambda} \tag{54e}$$

$$Y_{33} = \frac{v_E^2}{(R_\Phi + h)^2} + \frac{v_N^2}{(R_\lambda + h)^2} + \frac{\partial g}{\partial h} \tag{54f}$$

and

$$Z_{11} = \frac{v_D}{R_\lambda + h}, \quad Z_{12} = -\frac{2v_E \tan\lambda}{R_\Phi + h} + 2\omega_e \sin\lambda, \quad Z_{12} = \frac{v_N}{R_\lambda + h} \tag{55a}$$

$$Z_{21} = \frac{v_E \tan\lambda}{R_\Phi + h} + 2\omega_e \sin\lambda, \quad Z_{22} = \frac{v_D + v_N \tan\lambda}{R_\Phi + h}, \quad Z_{23} = \frac{v_E}{R_\Phi + h} + 2\omega_e \cos\lambda \tag{55b}$$

$$Z_{31} = -\frac{2v_N}{R_\lambda + h}, \quad Z_{32} = -\frac{2v_E}{R_\Phi + h} - 2\omega_e \cos\lambda \tag{55c}$$

with

$$\frac{\partial g}{\partial \lambda} = 9.780327[1.06048 \times 10^{-2} \sin\lambda\cos\lambda - 4.64 \times 10^{-5}(\sin\lambda\cos^3\lambda - \sin^3\lambda\cos\lambda)] + 8.8 \times 10^{-9} h\, \sin\lambda\cos\lambda \tag{56a}$$

$$\frac{\partial g}{\partial h} = -3.0877 \times 10^{-6} + 4.4 \times 10^{-9}\sin^2\lambda + 1.44 \times 10^{-13} h \tag{56b}$$

The GPS/INS estimation algorithm is summarized in Table 1. The assumed measurements are modelled by

$$\tilde{\mathbf{p}}_k = \mathbf{p}_k + \mathbf{v}_k \tag{57}$$

where $\mathbf{v}_k$ is a zero-mean Gaussian noise process with covariance given by R_k, which is provided from the solution of the GPS position determination problem coupled with the transformation given by Eq. (18). The filter is first initialized with a known state (the bias initial conditions for the gyro and accelerometer are usually assumed zero) and error-covariance matrix. The first three diagonal elements of the error-covariance matrix correspond to attitude errors. Then, the Kalman gain is computed using the measurement-error covariance R_k and sensitivity matrix. The state error-covariance follows the standard EKF update. The position, velocity and bias states also follow the standard EKF additive correction while the attitude error-state update is computed using a multiplicative update.[14] Also, the updated quaternion is re-normalized by brute force. Finally, the propagation equations follow the standard EKF model. The process noise covariance is given in Eq. (48), and the matrices F and G are given in Eq. (50).

In order to reduce the computational load a discrete-time propagation of the covariance matrix can be used, given by

$$P_{k+1}^- = \Phi_k P_k^+ \Phi_k^T + \mathcal{Q}_k \tag{58}$$

where Φ_k is the discrete-time state transition matrix and $\mathcal{Q}_k$ is the covariance matrix. A numerical solution for these matrices is given by van Loan.[18] First, the following $2n \times 2n$ matrix is formed:

$$\mathcal{A} = \begin{bmatrix} -F & G\,Q\,G^T \\ 0 & F^T \end{bmatrix} \Delta t \tag{59}$$

Table 1. Extended Kalman Filter for (Loose) GPS/INS Estimation

Initialize	$\hat{\mathbf{x}}(t_0) = \hat{\mathbf{x}}_0$ $P(t_0) = P_0$
Gain	$K_k = P_k^- H_k^T [H_k P_k^- H_k^T + R_k]^{-1}$ $H_k = \begin{bmatrix} 0_{3\times3} & I_{3\times3} & 0_{3\times3} & 0_{3\times3} & 0_{3\times3} & 0_{3\times3} & 0_{3\times3} \end{bmatrix}$
Update	$P_k^+ = [I - K_k H_k] P_k^-$ $\Delta\hat{\mathbf{x}}_k^+ = K_k[\tilde{\mathbf{p}}_k - \hat{\mathbf{p}}_k^-]$ $\hat{\mathbf{q}}_k^+ = \hat{\mathbf{q}}_k^- + \frac{1}{2}\Xi(\hat{\mathbf{q}}_k^-)\boldsymbol{\delta\hat{\alpha}}_k^+$, re-normalize quaternion $\hat{\mathbf{p}}_k^+ = \hat{\mathbf{p}}_k^- + \Delta\hat{\mathbf{p}}_k^+$ $\hat{\mathbf{v}}_k^{N+} = \hat{\mathbf{v}}_k^{N-} + \Delta\hat{\mathbf{v}}_k^{N+}$ $\hat{\mathbf{b}}_{g_k}^+ = \hat{\mathbf{b}}_{g_k}^- + \Delta\hat{\mathbf{b}}_{g_k}^+$ $\hat{\mathbf{b}}_{a_k}^+ = \hat{\mathbf{b}}_{a_k}^- + \Delta\hat{\mathbf{b}}_{a_k}^+$ $\hat{\mathbf{k}}_{g_k}^+ = \hat{\mathbf{k}}_{g_k}^- + \Delta\hat{\mathbf{k}}_{g_k}^+$ $\hat{\mathbf{k}}_{a_k}^+ = \hat{\mathbf{k}}_{a_k}^- + \Delta\hat{\mathbf{k}}_{a_k}^+$
Propagation	$\hat{\boldsymbol{\omega}}_{B/N}^B = (I_{3\times3} - \hat{\mathcal{K}}_g)(\tilde{\boldsymbol{\omega}}_{B/I}^B - \hat{\mathbf{b}}_g) - A_N^B(\hat{\mathbf{q}})\boldsymbol{\omega}_{N/I}^N$ $\dot{\hat{\mathbf{q}}} = \frac{1}{2}\Xi(\hat{\mathbf{q}})\,\hat{\boldsymbol{\omega}}_{B/N}^B$ $\hat{\mathbf{a}}^B = (I_{3\times3} - \hat{\mathcal{K}}_a)(\tilde{\mathbf{a}}^B - \hat{\mathbf{b}}_a)$ $\dot{\hat{\mathbf{p}}} = \mathbf{f}_p(\hat{\mathbf{p}}, \hat{\mathbf{v}}^N)$ $\dot{\hat{\mathbf{v}}}^N = \mathbf{f}_v(\hat{\mathbf{p}}, \hat{\mathbf{v}}^N) + \hat{\mathbf{a}}^N$ $\dot{P} = F\,P + P\,F^T + G\,Q\,G^T$

where Δt is the constant sampling interval. Then, the matrix exponential of Eq. (59) is computed:

$$\mathcal{B} = e^{\mathcal{A}} \equiv \begin{bmatrix} \mathcal{B}_{11} & \mathcal{B}_{12} \\ 0 & \mathcal{B}_{22} \end{bmatrix} = \begin{bmatrix} \mathcal{B}_{11} & \Phi_k^{-1}\mathcal{Q}_k \\ 0 & \Phi_k^T \end{bmatrix} \tag{60}$$

The state transition matrix is then given by

$$\Phi_k = \mathcal{B}_{22}^T \tag{61}$$

Also, the discrete-time process noise covariance is given by

$$\mathcal{Q}_k = \Phi_k\,\mathcal{B}_{12} \tag{62}$$

Note, the first-order approximation of Eq. (62) is given by $\Delta t\,G\,Q\,G^T$.

VI. Unscented Filtering

In this section a new approach that has been developed by Julier, Uhlmann, and Durrant-Whyte[19] is shown as an alternative to the EKF. This approach, which they called the *Unscented filter* (UF), typically involves more computations than the EKF, but has several advantages, including: 1) the expected error is lower than the EKF, 2) the new filter can be applied to non-differentiable functions, 3) the new filter avoids the derivation of Jacobian matrices, and 4) the new filter is valid to higher-order expansions than the standard EKF. The UF works on the premise that with a fixed number of parameters it should be easier to approximate a Gaussian distribution than to approximate an arbitrary nonlinear function. The filter presented in Ref. 20 is derived for discrete-time nonlinear equations, where the system model is given by

$$\mathbf{x}_{k+1} = \mathbf{f}(\mathbf{x}_k, k) + \mathbf{w}_k \tag{63a}$$

$$\tilde{\mathbf{y}}_k = \mathbf{h}(\mathbf{x}_k, k) + \mathbf{v}_k \tag{63b}$$

Note that a continuous-time model can always be written using eqn. (63a) through an appropriate numerical integration scheme. It is assumed that $\mathbf{w}_k$ and $\mathbf{v}_k$ are zero-mean Gaussian noise processes with covariances given by $\mathcal{Q}_k$ and R_k, respectively. We first rewrite the Kalman filter update equations as[21]

$$\hat{\mathbf{x}}_k^+ = \hat{\mathbf{x}}_k^- + K_k \boldsymbol{\upsilon}_k \tag{64a}$$

$$P_k^+ = P_k^- - K_k P_k^{\upsilon\upsilon} K_k^T \tag{64b}$$

where $\boldsymbol{\upsilon}_k$ is the *innovations process*, given by

$$\begin{aligned} \boldsymbol{\upsilon}_k &\equiv \tilde{\mathbf{y}}_k - \hat{\mathbf{y}}_k^- \\ &= \tilde{\mathbf{y}}_k - \mathbf{h}(\hat{\mathbf{x}}_k^-,\, \mathbf{u}_k, k) \end{aligned} \tag{65}$$

The covariance of $\boldsymbol{\upsilon}_k$ is defined by $P_k^{\upsilon\upsilon}$. The gain K_k is computed by

$$K_k = P_k^{xy} (P_k^{\upsilon\upsilon})^{-1} \tag{66}$$

where P_k^{xy} is the cross-correlation matrix between $\hat{\mathbf{x}}_k^-$ and $\hat{\mathbf{y}}_k^-$.

The Unscented filter uses a different propagation than the form given by the standard extended Kalman filter. Given an $n \times n$ covariance matrix P, a set of order n points can be generated from the columns (or rows) of the matrices $\pm\sqrt{nP}$. The set of points is zero-mean, but if the distribution has mean $\boldsymbol{\mu}$, then simply adding $\boldsymbol{\mu}$ to each of the points yields a symmetric set of $2n$ points having the desired mean and covariance.[19] Due to the symmetric nature of this set, its odd central moments are zero, so its first three moments are the same as the original Gaussian distribution. This is the foundation for the UF.

A method for incorporating process noise in the UF is shown in Ref. 22. This approach generates a set of points in $[\mathbf{x}_k,\, \mathbf{w}_k]$ space that has the correct mean and covariance, and propagates these points through the model in Eq. (63a). The predicted mean and covariance are also augmented to included the process noise, but the basic structure of the their calculations remain unchanged (see Ref. 22 for more details). Although this approach may more fully utilize the capability of the unscented transformation, it will be more computationally costly due to the extra required calculations arising from the augmented system. This significantly increases the computational burden, which may prohibit its use for actual onboard implementations. Another approach based on a trapezoidal approximation will be shown here.

The general formulation for the propagation equations are given as follows. First, the following set of *sigma points* are computed:

$$\boldsymbol{\sigma}_k \leftarrow 2n \text{ columns from } \pm\gamma\sqrt{P_k^+ + \bar{Q}_k} \tag{67a}$$

$$\boldsymbol{\chi}_k(0) = \hat{\mathbf{x}}_k^+ \tag{67b}$$

$$\boldsymbol{\chi}_k(i) = \boldsymbol{\sigma}_k(i) + \hat{\mathbf{x}}_k^+ \tag{67c}$$

where the matrix $\bar{Q}_k$ is related to the process noise covariance, which will be discussed shortly. The parameter γ is given by

$$\gamma = \sqrt{n + \lambda} \tag{68}$$

where the composite scaling parameter, λ, is given by

$$\lambda = \alpha^2(n + \kappa) - n \tag{69}$$

The constant α determines the spread of the sigma points and is usually set to a small positive value (e.g., $1 \times 10^{-4} \leq \alpha \leq 1$).[20] Also, the significance of the parameter κ will be discussed shortly. One efficient method to compute the matrix square root is the Cholesky decomposition.[23] Alternatively, the sigma points can be chosen to lie along the eigenvectors of the covariance matrix. Note that there are a total of $2n$ values for $\boldsymbol{\sigma}_k$ (the positive and negative square roots). The transformed set of sigma points are evaluated for each of the points by

$$\boldsymbol{\chi}_{k+1}(i) = \mathbf{f}[\boldsymbol{\chi}_k(i), k] \tag{70}$$

We now define the following weights:

$$W_0^{\text{mean}} = \frac{\lambda}{n + \lambda} \tag{71a}$$

$$W_0^{\text{cov}} = \frac{\lambda}{n + \lambda} + (1 - \alpha^2 + \beta) \tag{71b}$$

$$W_i^{\text{mean}} = W_i^{\text{cov}} = \frac{1}{2(n + \lambda)}, \quad i = 1, 2, \ldots, 2n \tag{71c}$$

where β is used to incorporate prior knowledge of the distribution (a good starting guess is $\beta = 2$).

The predicted mean for the state estimate is calculated using a weighted sum of the points $\boldsymbol{\chi}^x_{k+1}(i)$, which is given by

$$\hat{\mathbf{x}}^-_{k+1} = \sum_{i=0}^{2n} W_i^{\text{mean}} \, \boldsymbol{\chi}_{k+1}(i) \tag{72}$$

The predicted covariance is given by

$$P^-_{k+1} = \sum_{i=0}^{2n} W_i^{\text{cov}} \left[\boldsymbol{\chi}_{k+1}(i) - \hat{\mathbf{x}}^-_{k+1}\right] \left[\boldsymbol{\chi}_{k+1}(i) - \hat{\mathbf{x}}^-_{k+1}\right]^T + \bar{Q}_k \tag{73}$$

The mean observation is given by

$$\hat{\mathbf{y}}^-_{k+1} = \sum_{i=0}^{2n} W_i^{\text{mean}} \, \boldsymbol{\gamma}_{k+1}(i) \tag{74}$$

where

$$\boldsymbol{\gamma}_{k+1}(i) = \mathbf{h}[\boldsymbol{\chi}_{k+1}(i), k+1] \tag{75}$$

The output covariance is given by

$$P^{yy}_{k+1} = \sum_{i=0}^{2n} W_i^{\text{cov}} \left[\boldsymbol{\gamma}_{k+1}(i) - \hat{\mathbf{y}}^-_{k+1}\right] \left[\boldsymbol{\gamma}_{k+1}(i) - \hat{\mathbf{y}}^-_{k+1}\right]^T \tag{76}$$

Then the innovations covariance is simply given by

$$P^{\upsilon\upsilon}_{k+1} = P^{yy}_{k+1} + R_{k+1} \tag{77}$$

Finally the cross correlation matrix is determined using

$$P^{xy}_{k+1} = \sum_{i=0}^{2n} W_i^{\text{cov}} \left[\boldsymbol{\chi}_{k+1}(i) - \hat{\mathbf{x}}^-_{k+1}\right] \left[\boldsymbol{\gamma}_{k+1}(i) - \hat{\mathbf{y}}^-_{k+1}\right]^T \tag{78}$$

The filter gain is then computed using eqn. (66), and the state vector can now be updated using eqn. (64). Even though propagations on the order of $2n$ are required for the Unscented filter, the computations may be comparable to the extended Kalman filter (especially if the continuous-time covariance equation needs to be integrated and a numerical Jacobian matrix is evaluated).

The scalar κ in the previous set of equations is a convenient parameter for exploiting knowledge (if available) about the higher moments of the given distribution.[21] In scalar systems (i.e., for $n = 1$), a value of $\kappa = 2$ leads to errors in the mean and variance that are sixth order. For higher-dimensional systems choosing $\kappa = 3 - n$ minimizes the mean-squared-error up to the fourth order.[19] However, caution should be exercised when κ is negative since a possibility exists that the predicted covariance can become non-positive semi-definite. A modified form has been suggested for this case (see Ref. 19). Also, a square root version of the Unscented filter is presented in Ref. 20 that avoids the need to re-factorize at each step. Furthermore, Ref. 20 presents an Unscented Particle filter, which makes no assumptions on the form of the probability densities, i.e., full nonlinear, non-Gaussian estimation.

Reference 22 states that if the process noise is purely additive in the model, then its covariance can simply be added using a simple additive procedure. In this paper we expand upon this concept by incorporating an approximation for the integration over the sampling interval, which more closely follows the actual process. Any process noise that is added to the state vector in the UF is effectively multiplied by the state transition matrix, $\Phi(\Delta t)$, which gives $\Phi(\Delta t)\, Q_k \Phi^T(\Delta t)$ at the end of the interval. This mapping is done automatically by the state propagation, and does not need to be explicitly accounted for in the propagation. However, adding equal process noise at the beginning and end of the propagation might yield better results. The total desired process noise follows

$$\Phi(\Delta t)\, \bar{Q}_k \Phi^T(\Delta t) + \bar{Q}_k = \mathcal{Q}_k \tag{79}$$

where $\bar{Q}_k$ is used in Eq. (67a) and in the calculation of the predicted covariance in Eq. (73). This approach is similar to a trapezoid rule for integration. Equation (79) is known as the discrete-time *Sylvester equation*.

A. Unscented GPS/INS Filter

In this section an UF is derived for GPS/INS estimation. This filter is straightforward, except for the quaternion normalization. Mainly, referring to Eq. (72), since the predicted quaternion mean is derived using an averaged sum of quaternions, no guarantees can be made that the resulting quaternion will have unit norm. This makes the straightforward implementation of the UF with quaternions undesirable. A better way involves using an unconstrained three-component vector to represent an attitude error quaternion. We begin by defining the following state vector:

$$\boldsymbol{\chi}_k(0) = \hat{\mathbf{x}}_k^+ \equiv \begin{bmatrix} \boldsymbol{\delta}\hat{\mathbf{s}}_k^+ \\ \hat{\mathbf{p}}_k^+ \\ \hat{\mathbf{v}}_k^{N+} \\ \hat{\mathbf{b}}_{g_k}^+ \\ \hat{\mathbf{b}}_{a_k}^+ \\ \hat{\mathbf{k}}_{g_k}^+ \\ \hat{\mathbf{k}}_{a_k}^+ \end{bmatrix}, \quad \boldsymbol{\chi}_k(i) \equiv \begin{bmatrix} \boldsymbol{\chi}_k^{\delta s}(i) \\ \boldsymbol{\chi}_k^{p}(i) \\ \boldsymbol{\chi}_k^{V^N}(i) \\ \boldsymbol{\chi}_k^{b_g}(i) \\ \boldsymbol{\chi}_k^{b_a}(i) \\ \boldsymbol{\chi}_k^{\mathcal{K}_g}(i) \\ \boldsymbol{\chi}_k^{\mathcal{K}_a}(i) \end{bmatrix} \tag{80}$$

where $\boldsymbol{\delta}\hat{\mathbf{s}}_k^+$ is a generalized Rodrigues error-vector[24] used to propagate and update a nominal quaternion. Since this three-dimensional representation is unconstrained, the resulting overall covariance matrix is a 21×21 matrix. Therefore, using Eq. (72) poses no difficulties, which makes this an attractive approach. Now, define the first three components of the vector $\boldsymbol{\chi}_k(i)$ in Eq. (67) as $\boldsymbol{\chi}_k^{\delta s}(i)$. To describe $\boldsymbol{\chi}_k^{\delta s}$ we first define a new quaternion generated by multiplying an error quaternion by the current estimate. Using the notation in Eq. (67) we assume

$$\hat{\mathbf{q}}_k^+(0) = \hat{\mathbf{q}}_k^+ \tag{81a}$$

$$\hat{\mathbf{q}}_k^+(i) = \boldsymbol{\delta}\mathbf{q}_k^+(i) \otimes \hat{\mathbf{q}}_k^+, \quad i = 1,\, 2,\, \ldots,\, 42 \tag{81b}$$

with $\boldsymbol{\delta}\mathbf{q}_k^+(i) \equiv \left[\boldsymbol{\delta}\boldsymbol{\varrho}_k^{+T}(i) \;\; \delta q_{4_k}^+(i)\right]^T$ represented by[24]

$$\delta q_{4_k}^+(i) = \frac{-a\,||\boldsymbol{\chi}_k^{\delta s}(i)||^2 + f\sqrt{f^2 + (1-a^2)||\boldsymbol{\chi}_k^{\delta s}(i)||^2}}{f^2 + ||\boldsymbol{\chi}_k^{\delta s}(i)||^2}, \quad i = 1,\, 2\,\ldots,\, 42 \tag{82a}$$

$$\boldsymbol{\delta}\boldsymbol{\varrho}_k^+(i) = f^{-1}\left[a + \delta q_{4_k}^+(i)\right]\, \boldsymbol{\chi}_k^{\delta s}(i), \quad i = 1,\, 2,\, \ldots,\, 42 \tag{82b}$$

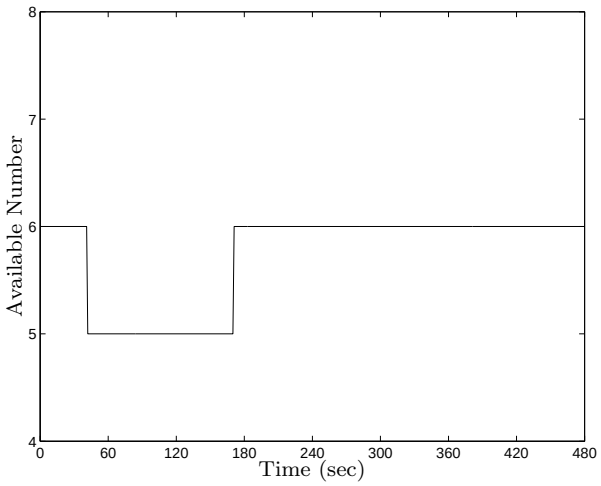

Figure 2. Number of Available GPS Satellites

where a is a parameter from 0 to 1, and f is a scale factor. Note when $a = 0$ and $f = 1$ then $\boldsymbol{\chi}_k^{\delta s}$ gives the Gibbs vector, and when $a = f = 1$ then $\boldsymbol{\chi}_k^{\delta s}$ gives the standard vector of modified Rodrigues parameters (MRPs). For small errors the attitude part of the covariance is closely related to the attitude estimation errors for any rotation sequence, given by a simple factor.[14] For example, the Gibbs vector linearize to half angles, and the vector of MRPs linearize to quarter angles. We will choose $f = 2(a + 1)$ so that $||\boldsymbol{\chi}_k^{\delta s}||$ is equal to the rotational error-angle for small errors. Equation (81a) clearly requires that $\boldsymbol{\chi}_k^{\delta s}(0)$ be zero. This is due to the reset of the attitude error to zero after the previous update, which is used to move information from one part of the estimate to another part.[25] This reset rotates the reference frame for the covariance, so we might expect the covariance to be rotated, even though no new information is added. But the covariance depends on the assumed statistics of the measurements, not on the actual measurements. Therefore, since the update is zero-mean, the mean rotation caused by the reset is actually zero, so the covariance is in fact not affected by the reset. Next, the updated quaternions are propagated forward using Eq. (40a), with

$$\dot{\hat{\mathbf{q}}}(i) = \frac{1}{2}\Xi[\hat{\mathbf{q}}(i)]\hat{\boldsymbol{\omega}}_{B/N}^{B}(i), \quad i = 0,\, 1,\, \ldots,\, 42 \tag{83}$$

with the estimated angular velocities given by

$$\hat{\boldsymbol{\omega}}_{B/N}^{B}(i) = [I_{3\times 3} - \boldsymbol{\chi}^{\mathcal{K}_g}(i)]\left[\tilde{\boldsymbol{\omega}}_{B/I}^{B} - \boldsymbol{\chi}^{b_g}(i)\right] - A_N^B[\hat{\mathbf{q}}(i)]\boldsymbol{\omega}_{N/I}^{N}, \quad i = 0,\, 1,\, \ldots,\, 42 \tag{84}$$

where $\boldsymbol{\chi}^{\mathcal{K}_g}(i)$ and $\boldsymbol{\chi}^{b_g}(i)$ are formed from the gyro scale-factor and bias sigma points, respectively. The propagated error quaternions are computed using

$$\boldsymbol{\delta}\mathbf{q}_{k+1}^{-}(i) = \hat{\mathbf{q}}_{k+1}^{-}(i) \otimes \left[\hat{\mathbf{q}}_{k+1}^{-}(0)\right]^{-1}, \quad i = 0,\, 1,\, \ldots,\, 42 \tag{85}$$

Note that $\boldsymbol{\delta}\mathbf{q}_{k+1}^{-}(0)$ is the identity quaternion. Finally, the propagated sigma points can be computed using[24]

$$\boldsymbol{\chi}_{k+1}^{\delta s}(0) = \mathbf{0} \tag{86a}$$

$$\boldsymbol{\chi}_{k+1}^{\delta s}(i) = f\frac{\boldsymbol{\delta\varrho}_{k+1}^{-}(i)}{a + \delta q_{4_{k+1}}^{-}(i)}, \quad i = 1,\, 2,\, \ldots,\, 42 \tag{86b}$$

with $\left[\boldsymbol{\delta\varrho}_{k+1}^{-T}(i) \;\; \delta q_{4_{k+1}}^{-}(i)\right]^T = \boldsymbol{\delta}\mathbf{q}_{k+1}^{-}(i)$. The predicted mean and covariance can now be computed using Eqs. (72) and (73).

The procedure in the Unscented GPS/INS filter is as follows. We are given initial estimates for the attitude, position, velocity, and biases and scale factors, as well as an initial 21×21 covariance (P_0^+), where

the upper 3×3 partition of P_0^+ corresponds to attitude error angles. The first three components of the initial state vector in the UF is set to zero and the others are set to their initial values for position, velocity, biases and scale factors. We choose the parameter a and set $f = 2(a+1)$. Then, $\bar{Q}_k$ is calculated using Eq. (79), which will be used in Eqs. (67a) and (73), where Φ_k is given by Eq. (61) and $\mathcal{Q}_k$ is given by Eq. (62). The sigma points are then calculated using Eq. (67). Next, the corresponding error quaternions are calculated using Eq. (82), where Eq. (81) is used to compute the sigma-point quaternions from the error quaternions. The quaternions are subsequently propagated forward in time using Eq. (83). Then, the propagated error quaternions are determined using Eq. (85), and the propagated sigma points are calculated using Eq. (86). All other sigma-point quantities, such as position, velocity, biases and scale factors, are propagated using Eq. (40). The predicted mean and covariance can now be computed using Eqs. (72) and (73). Storing the propagated quaternions from Eq. (83) we then calculate the mean observations using Eqs. (74) and (75). The output covariance, innovation covariance and cross-correlation matrix are computed using Eqs. (76), (77) and (78). Next, the state vector and covariance are updated using Eq. (64). Then, the quaternion is updated using

$$\hat{\mathbf{q}}_{k+1}^{+} = \boldsymbol{\delta}\mathbf{q}_{k+1}^{+} \otimes \hat{\mathbf{q}}_{k+1}^{-}(0) \tag{87}$$

where $\boldsymbol{\delta}\mathbf{q}_{k+1}^{+} \equiv \begin{bmatrix} \boldsymbol{\delta}\boldsymbol{\varrho}_{k+1}^{+T} & \delta q_{4_{k+1}}^{+} \end{bmatrix}^T$ is represented by[24]

$$\delta q_{4_{k+1}}^{+} = \frac{-a\,||\boldsymbol{\delta}\hat{\mathbf{s}}_{k+1}^{+}||^2 + f\sqrt{f^2 + (1-a^2)||\boldsymbol{\delta}\hat{\mathbf{s}}_{k+1}^{+}||^2}}{f^2 + ||\boldsymbol{\delta}\hat{\mathbf{s}}_{k+1}^{+}||^2} \tag{88a}$$

$$\boldsymbol{\delta}\boldsymbol{\varrho}_{k+1}^{+} = f^{-1}\left[a + \delta q_{4_{k+1}}^{+}\right]\boldsymbol{\delta}\hat{\mathbf{s}}_{k+1}^{+} \tag{88b}$$

Finally, $\boldsymbol{\delta}\hat{\mathbf{s}}_{k+1}^{+}$ is reset to zero for the next propagation.

VII. Simulation Results

In this section simulation results are shown that estimate for a moving vehicle's attitude, position and velocity, as well as the gyro and accelerometer biases and scale factors. All measurements are assumed to be sampled every 1 second. The total time of the simulation is 8 minutes. The gyro noise parameters are given by $\sigma_{gv} = 2.9089\times10^{-7}$ rad/sec$^{1/2}$ and $\sigma_{gu} = 9.1989\times10^{-7}$ rad/sec$^{3/2}$. The accelerometer parameters are given by $\sigma_{av} = 9.8100\times10^{-5}$ m/sec$^{3/2}$ and $\sigma_{au} = 6.0000\times10^{-5}$ m/sec$^{5/2}$. Initial biases for the gyros and accelerometers are given by 10 deg/hr and 0.003 m/s^2, respectively, for each axis. Also, $\mathcal{K}_g = 0.01I_{3\times3}$ and $\mathcal{K}_a = 0.005I_{3\times3}$. The vehicle motion is described in NED coordinates with the origin (point of interest) location at $\lambda_0 = 38^\circ$ and $\Phi_0 = -77^\circ$. The initial quaternion is given so that the vehicle body frame is aligned with the local NED frame. The initial velocity is given by $\mathbf{v}_0^N = [200\ \ 200\ \ -10]^T$ m/s. The acceleration inputs are given by $a_N = 0$, $a_E = 0$ and $a_D = -g_0$, where g_0 is the initial gravity. The rotational rate profile is given by: 5 deg/min rotation about the x axis for the first 160 seconds and then zero for the final 320 seconds; no rotation about the y axis for the first 160 seconds, then a 5 deg/min rotation for the next 160 seconds and zero for the final 160 seconds; no rotation about the z axis for the first 320 seconds, then 5 deg/min rotation for the final 160 seconds. The GPS constellation is simulated using GPS week 137 and a time of applicability of 61440.0000 seconds (see Ref. 11 for an explanation of GPS time). Using the position profile the number of GPS satellites available can be computed using a 15° elevation cutoff.[11] The number of available GPS satellites over time is shown in Figure 2, which ranges from a minimum of 5 satellites to a maximum of 6 satellites. The clock-bias drift is modelled using a random walk process: $\dot{\tau} = w_\tau$, where the variance (in seconds) of w_τ is given by 200. GPS measurements are obtained using a standard deviation of 5 meters for the white-noise errors.

Using all available GPS pseudoranges an ECEF position is determined using nonlinear least squares, which is then converted into longitude, latitude and height using Eq. (4). These quantities are used as "measurements" in the filters with covariance computed using Eq. (18), where $P_{\text{pos}}^{\text{ECEF}}$ is computed from the nonlinear least square solution. The approach corresponds to a "loose" GPS/INS configuration. In general, position is very well known but attitude is not. To test the robustness of the EKF an initial attitude error of 15 degrees is given in each axis. This error is not unrealistic for an actual application. The initial covariance matrix P_0 in the EKF is diagonal. For this case, the three attitude parts of the initial covariance are each set to a 3σ bound of 15 degrees, i.e., $[(15/3)\times(\pi/180)]^2$ rad^2. The initial estimates for position are set

to the true latitude, longitude and height. The initial variances for latitude and longitude are each given by $(1 \times 10^{-6})^2$ rad^2. The initial variance for height is given by $(20/3)^2$ m^2. To further stress the filters the initial velocity is set to zero. For this case, the initial variances in the filters for v_N and v_E are each set to $(200/3)^2$ and the initial variance for v_D is set to $(10/3)^2$. The initial gyro and accelerometer biases and scale factors are all set to zero. The three gyro-bias parts of the initial covariance are each set to a 3σ bound of 30 degrees per hour, i.e., $[(30/3) \times (\pi/(180 \times 3600))]^2$. The three accelerometer-bias parts of the initial covariance are each set to a 3σ bound of 0.005 meters per second-squared, i.e., $(0.005/3)^2$. The three gyro-scale factor parts of the initial covariance are each set to a 3σ bound of 0.015, i.e., $(0.015/3)^2$. Finally, the three accelerometer-scale factor parts of the initial covariance are each set to a 3σ bound of 0.010, i.e., $(0.010/3)^2$. The parameters used in the UF are given by $\alpha = 0.003$, $\beta = 2$ and $\kappa = 3 - n$, where $n = 21$.

The resulting EKF attitude errors for a typical case are shown in Figure 3(a). The attitude errors diverge and significantly drift outside their respective 3σ bounds, which indicates that the EKF is performing in a subpar fashion. This is due to the large initial errors that are not handled well in the linearization of the dynamic model in the EKF. However, the UF attitude errors are much closer to their respective 3σ bounds than the EKF attitude errors, as shown in Figure 3(b). The larger errors in yaw are due to the fact that this angle is the least observable state for the particular vehicle motion. The biggest concern with the EKF solutions is the confidence of the results dictated by the 3σ bounds. In fact, if the truth is not known *a prior* and we only had the covariance to assess filter performance, this plot would indicate that the EKF is performing better than the UF. This can certainly provide some misleading results when using the EKF with large initial condition errors. The position errors for the EKF are given by Figure 3(c). The latitude and height errors remain within their respective 3σ bounds for the entire simulation run, but longitude drifts outside the bound for a small period. This is a surprising result for the EKF since position measurements are directly used in the filter. However, all UF position errors remain inside their respective 3σ bounds. A comparison of the gyro bias estimates between the EKF and UF is shown by Figures 3(e) and 3(f), respectively. The errors for the EKF drift outside of their respected 3σ bounds for every axis. However, the UF bias errors are much closer to their 3σ bounds than the EKF bias errors, as shown in Figure 3(f). These simulation results clearly indicate that the UF is able to provide more robust characteristics than an EKF for GPS/INS applications.

VIII. Conclusions

In this paper an Unscented filter formulation was derived for the purpose of GPS/INS applications. The filter is based on a quaternion parameterization of the attitude. However, straightforward implementation of the Unscented filter using quaternion kinematics did not produce a unit quaternion estimate. To overcome this difficulty the quaternion was represented by a three-dimensional vector of generalized Rodrigues parameters, which also reduced the size the covariance matrix. Simulation results indicated that the performance of the Unscented filter exceeds the standard extended Kalman filter for large initialization errors.

Acknowledgements

This work was funded by the DOE NNSA NA-22 Proliferation Detection Program Office, Advanced Radar Systems project, under the guidance of Theodore Kim and Curtis Webb at Sandia National Laboratories. The author greatly appreciates this support. Also, the author wishes to thank F. Landis Markley from NASA Goddard Space Flight Center for numerous discussions on gyro noise modelling throughout the years.

References

[1]Chatfield, A. B., *Fundamentals of High Accuracy Inertial Navigation*, American Institute of Aeronautics and Astronautics, Inc., Reston, VA, 1997.

[2]Connelly, J., Kourepenis, A., Marinis, T., and Hanson, D., "Micromechanical Sensors in Tactical GN&C Applications," *AIAA Guidance, Navigation and Contol Conference*, Montreal, QB, Canada, Aug. 2001, AIAA-2001-4407.

[3]Farrell, J. and Barth, M., *The Global Positioning System & Inertial Navigation*, McGraw-Hill, New York, NY, 1998.

[4]Jekeli, C., *Inertial Navigation Systems with Geodetic Applications*, Walter de Gruyter, Berlin, Germany, 2000.

[5]Julier, S. J., Uhlmann, J. K., and Durrant-Whyte, H. F., "A New Method for the Nonlinear Transformation of Means and Covariances in Filters and Estimators," *IEEE Transactions on Automatic Control*, Vol. AC-45, No. 3, March 2000, pp. 477–482.

[6]van der Merwe, R., Wan, E. A., and Julier, S. I., "Sigma-Point Kalman Filters for Nonlinear Estimation and Sensor-

Fusion: Applications to Integrated Navigation," *AIAA Guidance, Navigation and Contol Conference*, Providence, RI, Aug. 2004, AIAA-2004-5120.

[7]Crassidis, J. L. and Junkins, J. L., *Optimal Estimation of Dynamic Systems*, Chapman & Hall/CRC, Boca Raton, FL, 2004.

[8]Bate, R. R., Mueller, D. D., and White, J. E., *Fundamentals of Astrodynamics*, Dover Publications, New York, NY, 1971.

[9]Wertz, J. R., "Space-Based Orbit, Attitude and Timing Systems," *Mission Geometry: Orbit and Constellation Design and Management*, chap. 4, Microcosm Press, El Segundo, CA and Kluwer Academic Publishers, The Netherlands, 2001.

[10]Meeus, J., *Astronomical Algorithms*, Willman-Bell, Inc., Richmond, VA, 2nd ed., 1999.

[11]Hofmann-Wellenhof, B., Lichtenegger, H., and Collins, J., *GPS: Theory and Practice*, Springer Wien, New York, NY, 5th ed., 2001.

[12]Shuster, M. D., "A Survey of Attitude Representations," *Journal of the Astronautical Sciences*, Vol. 41, No. 4, Oct.-Dec. 1993, pp. 439–517.

[13]Hamilton, W. R., *Elements of Quaternions*, Longmans, Green and Co., London, England, 1866.

[14]Lefferts, E. J., Markley, F. L., and Shuster, M. D., "Kalman Filtering for Spacecraft Attitude Estimation," *Journal of Guidance, Control, and Dynamics*, Vol. 5, No. 5, Sept.-Oct. 1982, pp. 417–429.

[15]Shepperd, S. W., "Quaternion from Rotation Matrix," *Journal of Guidance and Control*, Vol. 1, No. 3, May-June 1978, pp. 223–224.

[16]Kuipers, J. B., *Quaternions and Rotation Sequences: A Primer with Applications to Orbits, Aerospace, and Virtual Reality*, Princeton University Press, Princeton, NJ, 1999.

[17]Kim, S.-G., Crassidis, J. L., Cheng, Y., Fosbury, A. M., and Junkins, J. L., "Kalman Filtering for Relative Spacecraft Attitude and Position Estimation," *AIAA Guidance, Navigation and Contol Conference*, San Francisco, CA, Aug. 2005, AIAA-2005-6087.

[18]van Loan, C. F., "Computing Integrals Involving the Matrix Exponential," *IEEE Transactions on Automatic Control*, Vol. AC-23, No. 3, June 1978, pp. 396–404.

[19]Julier, S. J., Uhlmann, J. K., and Durrant-Whyte, H. F., "A New Approach for Filtering Nonlinear Systems," *Proceedings of the American Control Conference*, Seattle, WA, June 1995, pp. 1628–1632.

[20]Wan, E. and van der Merwe, R., "The Unscented Kalman Filter," *Kalman Filtering and Neural Networks*, edited by S. Haykin, chap. 7, Wiley, 2001.

[21]Bar-Shalom, Y. and Fortmann, T. E., *Tracking and Data Association*, Academic Press, Boston, MA, 1988, pp. 56–58.

[22]Wan, E. and van der Merwe, R., "The Unscented Kalman Filter," *Kalman Filtering and Neural Networks*, edited by S. Haykin, chap. 7, John Wiley & Sons, New York, NY, 2001.

[23]Golub, G. H. and Van Loan, C. F., *Matrix Computations*, The Johns Hopkins University Press, Baltimore, MD, 2nd ed., 1989, pp. 145–146.

[24]Crassidis, J. L. and Markley, F. L., "Unscented Filtering for Spacecraft Attitude Estimation," *Journal of Guidance, Control, and Dynamics*, Vol. 26, No. 4, July-Aug. 2003, pp. 536–542.

[25]Markley, F. L., "Attitude Representations for Kalman Filtering," *AAS/AIAA Astrodynamics Specialist Conference*, Quebec City, Quebec, Aug. 2001, AAS 01-309.

[26]Grewal, M. S., Weill, L. R., and Andrews, A. P., *Global Positioning Systems, Inertial Navigation, and Integration*, John Wiley & Sons, New York, NY, 2001.

[27]Farrenkopf, R. L., "Analytic Steady-State Accuracy Solutions for Two Common Spacecraft Attitude Estimators," *Journal of Guidance and Control*, Vol. 1, No. 4, July-Aug. 1978, pp. 282–284.

Appendix

In this appendix the gyro noise model is described in more detail.[‡] The single-axis gyro model with no scale factor correction is given by

$$\tilde{\omega}(t) = \omega(t) + b(t) + \eta_v(t) \tag{89a}$$

$$\dot{b}(t) = \eta_u(t) \tag{89b}$$

Dividing Eq. (89a) by Δt and integrating gives

$$\frac{1}{\Delta t}\int_{t_0}^{t_0+\Delta t} \tilde{\omega}(t)\ dt = \frac{1}{\Delta t}\int_{t_0}^{t_0+\Delta t} \left[\omega(t) + b(t) + \eta_v(t)\right]\ dt \tag{90}$$

Assuming that the measurement and truth are each constant over the interval (note: we cannot make the same assumption for the stochastic variables) yields

$$\tilde{\omega}(t_0+\Delta t) = \omega(t_0+\Delta t) + \frac{1}{\Delta t}\int_{t_0}^{t_0+\Delta t} \left[b(t) + \eta_v(t)\right]\ dt \tag{91}$$

[‡]This model is derived from notes provided by F. Landis Markley of NASA Goddard Space Flight Center.

Integrating Eq. (89b) gives

$$b(t_0 + \Delta t) = b(t_0) + \int_{t_0}^{t_0+\Delta t} \eta_u(t)\ dt \tag{92}$$

The variance of the gyro drift bias is given by

$$E\left\{b^2(t_0 + \Delta t)\right\} = E\left\{\left[b(t_0) + \int_{t_0}^{t_0+\Delta t} \eta_u(t)\ dt\right]\left[b(t_0) + \int_{t_0}^{t_0+\Delta t} \eta_u(\tau)\ d\tau\right]\right\} \tag{93}$$

Using $E\left\{\eta_u(t)\eta_u(\tau)\right\} = \sigma_u^2\,\delta(t-\tau)$ gives

$$E\left\{b^2(t_0 + \Delta t)\right\} = E\left\{b^2(t_0)\right\} + \sigma_u^2\,\Delta t \tag{94}$$

Therefore, the bias can be simulated using

$$b_m(t_0 + \Delta t) = b_m(t_0) + \sigma_u\,\Delta t^{1/2} N_u \tag{95}$$

where the subscript m denotes a modelled quantity and N_u is a zero-mean random variable with unit variance.

The bias at time t is given by

$$b(t) = b(t_0) + \int_{t_0}^{t} \eta_u(\tau)\ d\tau \tag{96}$$

Substituting Eq. (96) into Eq. (91) gives

$$\tilde{\omega}(t_0 + \Delta t) = z + \frac{1}{\Delta t}\int_{t_0}^{t_0+\Delta t}\int_{t_0}^{t} \eta_u(\tau)\ d\tau\ dt + \frac{1}{\Delta t}\int_{t_0}^{t_0+\Delta t} \eta_v(t)\ dt \tag{97}$$

where $z \equiv \omega(t_0 + \Delta t) + b(t_0)$. The correlation between the drift and rate measurement is given by

$$\begin{aligned} E\left\{b(t_0 + \Delta t)\,\tilde{\omega}(t_0 + \Delta t)\right\} = E\Bigg\{&\left[b(t_0) + \int_{t_0}^{t_0+\Delta t} \eta_u(\tau)\ d\tau\right] \\ &\times \left[\omega(t_0 + \Delta t) + b(t_0) + \frac{1}{\Delta t}\int_{t_0}^{t_0+\Delta t}\int_{t_0}^{t} \eta_u(\zeta)\ d\zeta\ dt + \frac{1}{\Delta t}\int_{t_0}^{t_0+\Delta t} \eta_v(t)\ dt\right]\Bigg\} \end{aligned} \tag{98}$$

Since $\eta_u(t)$ and $\eta_v(t)$ are uncorrelated we have

$$\begin{aligned} E\left\{b(t_0 + \Delta t)\,\tilde{\omega}(t_0 + \Delta t)\right\} &= E\left\{z\,b(t_0)\right\} + \frac{\sigma_u^2}{\Delta t}\int_{t_0}^{t_0+\Delta t}\int_{t_0}^{t_0+\Delta t}\int_{t_0}^{t} \delta(\tau-\zeta)\ d\zeta\ d\tau\ dt \\ &= E\left\{z\,b(t_0)\right\} + \frac{\sigma_u^2}{\Delta t}\int_{t_0}^{t_0+\Delta t} (t - t_0)\ dt \\ &= E\left\{z\,b(t_0)\right\} + \frac{1}{2}\sigma_u^2\,\Delta t \end{aligned} \tag{99}$$

Equation (99) can be satisfied by modelling the gyro measurement using

$$\tilde{\omega}_m(t_0 + \Delta t) = \omega_m(t_0 + \Delta t) + b_m(t_0) + \frac{1}{2}\sigma_u\,\Delta t^{1/2} N_u + c\,N_v \tag{100}$$

where c is yet to be determined and N_v is a zero-mean random variable with unit variance. Note that Eq. (100) can be proven by evaluating $E\left\{b_m(t_0 + \Delta t)\,\tilde{\omega}_m(t_0 + \Delta t)\right\}$. Solving Eq. (95) for N_u and substituting the resultant into Eq. (100) yields

$$\tilde{\omega}_m(t_0 + \Delta t) = \omega_m(t_0 + \Delta t) + \frac{1}{2}[b_m(t_0 + \Delta t) + b_m(t_0)] + c\,N_v \tag{101}$$

Note that $\frac{1}{2}[b_m(t_0 + \Delta t) + b_m(t_0)]$ is the "average" of the bias at the two times. This term is present due to the fact that the trapezoid rule for integration is exact for linear systems. To evaluate c we compute the

variance of the rate measurement:

$$E\left\{\tilde{\omega}^2(t_0+\Delta t)\right\} = E\left\{\left[z + \frac{1}{\Delta t}\int_{t_0}^{t_0+\Delta t}\int_{t_0}^{\tau}\eta_u(\upsilon)\ d\upsilon\ d\tau + \frac{1}{\Delta t}\int_{t_0}^{t_0+\Delta t}\eta_v(\tau)\ d\tau\right]\right.$$
$$\left.\times\left[z + \frac{1}{\Delta t}\int_{t_0}^{t_0+\Delta t}\int_{t_0}^{t}\eta_u(\zeta)\ d\zeta\ dt + \frac{1}{\Delta t}\int_{t_0}^{t_0+\Delta t}\eta_v(t)\ dt\right]\right\} \tag{102}$$

Since $\eta_u(t)$ and $\eta_v(t)$ are uncorrelated and using $E\left\{\eta_v(t)\eta_v(\tau)\right\} = \sigma_v^2\,\delta(t-\tau)$, then Eq. (102) simplifies to

$$E\left\{\tilde{\omega}^2(t_0+\Delta t)\right\} = E\left\{z^2\right\} + \frac{\sigma_u^2}{\Delta t^2}\int_{t_0}^{t_0+\Delta t}\int_{t_0}^{t_0+\Delta t}\int_{t_0}^{t}\int_{t_0}^{\tau}\delta(\upsilon-\zeta)\ d\upsilon\ d\zeta\ d\tau\ dt$$
$$+\frac{\sigma_v^2}{\Delta t^2}\int_{t_0}^{t_0+\Delta t}\int_{t_0}^{t_0+\Delta t}\delta(t-\tau)\ d\tau\ dt \tag{103}$$

The second to last integral can be computed by the following steps:

$$\begin{aligned}
&\int_{t_0}^{t_0+\Delta t}\int_{t_0}^{t_0+\Delta t}\int_{t_0}^{t}\int_{t_0}^{\tau}\delta(\upsilon-\zeta)\ d\upsilon\ d\zeta\ d\tau\ dt\\
&= \int_{t_0}^{t_0+\Delta t}\int_{t_0}^{t_0+\Delta t}\min(\tau-t_0,\, t-t_0)\ d\tau\ dt\\
&= \int_{t_0}^{t_0+\Delta t}\int_{t_0}^{t_0+\Delta t}\min(x,\, y)\ dx\ dy\\
&= \int_{0}^{\Delta t}\left(\int_{0}^{y}x\ dx + \int_{y}^{\Delta t}y\ dx\right)dy\\
&= \int_{0}^{\Delta t}\left[\frac{1}{2}y^2 + y(\Delta t - y)\right]\ dy\\
&= \frac{1}{3}\Delta t^3
\end{aligned} \tag{104}$$

Therefore, Eq. (103) reduces down to

$$E\left\{\tilde{\omega}^2(t_0+\Delta t)\right\} = E\left\{z^2\right\} + \frac{1}{3}\sigma_u^2\,\Delta t + \frac{\sigma_v^2}{\Delta t} \tag{105}$$

The variance of the modelled rate measurement in Eq. (100) is given by

$$E\left\{\tilde{\omega}_m^2(t_0+\Delta t)\right\} = E\left\{z_m^2\right\} + \frac{1}{4}\sigma_u^2\,\Delta t + c^2 \tag{106}$$

Comparing Eq. (106) to Eq. (105) gives

$$c^2 = \frac{\sigma_v^2}{\Delta t} + \frac{1}{12}\sigma_u^2\,\Delta t \tag{107}$$

Hence, the modelled rate measurement is given by

$$\tilde{\omega}_m(t_0+\Delta t) = \omega_m(t_0+\Delta t) + \frac{1}{2}[b_m(t_0+\Delta t) + b_m(t_0)] + \left[\frac{\sigma_v^2}{\Delta t} + \frac{1}{12}\sigma_u^2\,\Delta t\right]^{1/2} N_v \tag{108}$$

Generalizing Eqs. (95) and (108) for all times and dropping the subscript m gives the following formulas for the discrete-time rate and bias equations

$$\tilde{\omega}_{k+1} = \omega_{k+1} + \frac{1}{2}[b_{k+1} + b_k] + \left[\frac{\sigma_v^2}{\Delta t} + \frac{1}{12}\sigma_u^2\,\Delta t\right]^{1/2} N_v \tag{109a}$$

$$b_{k+1} = b_k + \sigma_u\,\Delta t^{1/2} N_u \tag{109b}$$

These equations are valid for both gyro and accelerometer measurements.

We now discuss other aspects of gyro and accelerometer specifications and how they relate to the INS EKF equations. We first discuss units. Unfortunately, specifications (and units) seem to vary from manufacturer to manufacturer. There are a number of various definitions for the term "bias" as well. Grewal et al.[26] give an explanation of these various definitions. There is a *fixed bias* that only needs to be calibrated once, a *bias stability* that varies from turn-on to turn-on due to thermal cycling among other causes, a *bias drift* after turn-on, and other biases that are g-dependent and shock dependent. The PSD σ_v^2 is often referred to as the *angle random walk*, which is a bit misleading. Also, σ_u^2 is sometimes referred to as the *rate random walk*. Many manufacturers give σ_v in units of deg/sqrt(hr) and a conversion to rad/sqrt(sec) is simple. Some manufacturers give the "random noise" units as deg/hr/sqrt(Hz). Both values are equivalent; if the second value is divided by 60 units of deg/sqrt(hr) are obtained:

$$\frac{\text{deg}}{\text{hr}\sqrt{\text{Hz}}} = \frac{\text{deg}}{\text{hr}\sqrt{\frac{1}{\text{sec}} \times \frac{3600\text{sec}}{1\text{ hr}}}} = \frac{\text{deg}}{60\text{hr}\sqrt{\frac{1}{\text{hr}}}} = \frac{\text{deg}}{60\sqrt{\text{hr}}} \tag{110}$$

The random noise of an accelerometer is often given in units of micro-g/sqrt(Hz). The conversion of these units into meters/sec$^{3/2}$ is given by

$$\frac{\mu\text{meters}}{\text{sec}^2\sqrt{\text{Hz}}} = \frac{\text{meters} \times 10^{-6}}{\text{sec}^2\sqrt{\frac{1}{\text{sec}}}} = \frac{\text{meters} \times 10^{-6}}{\text{sec}^{3/2}} \tag{111}$$

A small number of manufacturers will give rate changes and integrated output changes over time. The conversion of these parameters to σ_u and σ_v is given in Ref. 27. Suppose we are given a rate change of x rad/sec (1σ) in t_x hours. Then σ_u is given by

$$\sigma_u = \frac{x}{60\sqrt{t_x}} \quad \text{rad/sec}^{3/2} \tag{112}$$

Next, suppose we are given an integrated output change of y rad (1σ) in t_y hours. Then σ_v is given by

$$\sigma_v = \sqrt{\frac{y^2 - \frac{1}{3}\sigma_u^2 \times (3600\, t_y)^3}{3600\, t_y}} \quad \text{rad/sec}^{1/2} \tag{113}$$

where σ_u^2 is calculated using Eq. (112).

A more general model is given by

$$\tilde{\omega}(t) = (1+\kappa)\,\omega(t) + b(t) + d + \eta_v(t) \tag{114a}$$

$$\dot{b}(t) = -\alpha\, b(t) + \eta_u(t) \tag{114b}$$

$$\dot{d}(t) = 0 \tag{114c}$$

$$\dot{\kappa}(t) = 0 \tag{114d}$$

where κ is a "scale factor" and and the processes in Eqs. (114c) and (114c) are "random constants". Oftentimes the variance of d and κ are given by manufacturers as the "bias repeatability" and "scale factor error", respectively. The bias repeatability can be used to set $b(t_0)$. The units for the scale factor error are often given in "parts per million" (ppm). To determine the standard deviation of κ multiply ppm by 1×10^{-6}. The process in Eq. (114b) is called a *Markov process*, where $1/\alpha$ is the "correlation time". The variance of $\eta_u(t)$ is written as[4]

$$E\left\{\eta_u(t)\eta_u(\tau)\right\} = 2\,\sigma^2\alpha\,\delta(t-\tau) \equiv \sigma_u^2\,\delta(t-\tau) \tag{115}$$

where σ^2 is just another parameter. Note that for gyros the units of σ^2 are often given by deg/hr and for accelerometers in mgal, where 1 mgal $= 10^{-5}$ m/s^2 (1 gal $= 10^{-2}$ m/s^2). Hence, given the "correlated noise" parameters σ^2 and $1/\alpha$, then $\sigma_u^2 = 2\,\sigma^2\alpha$.

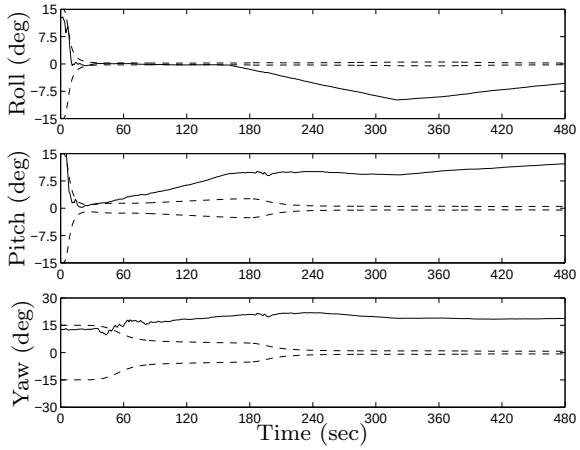

(a) EKF Attitude Errors and 3σ Bounds

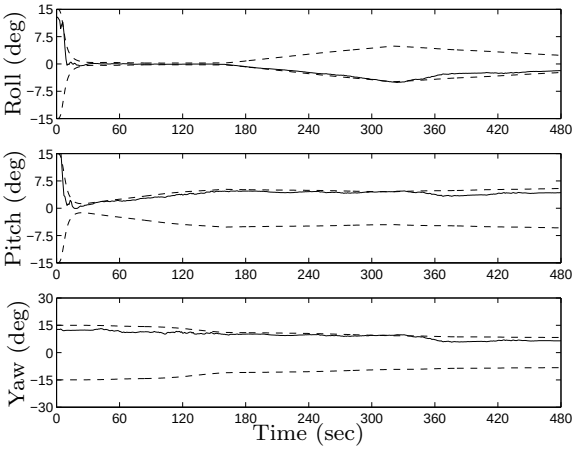

(b) UF Attitude Errors and 3σ Bounds

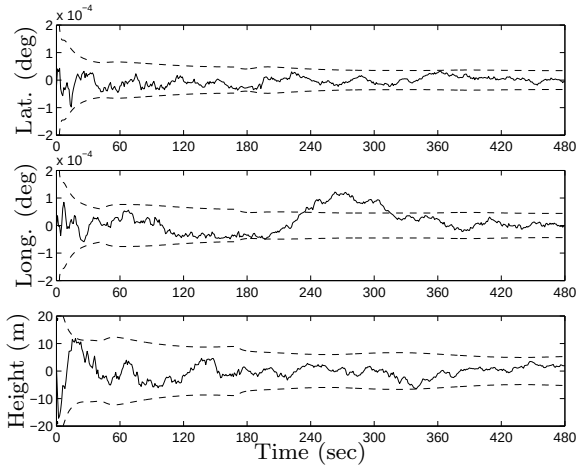

(c) EKF Position Errors and 3σ Bounds

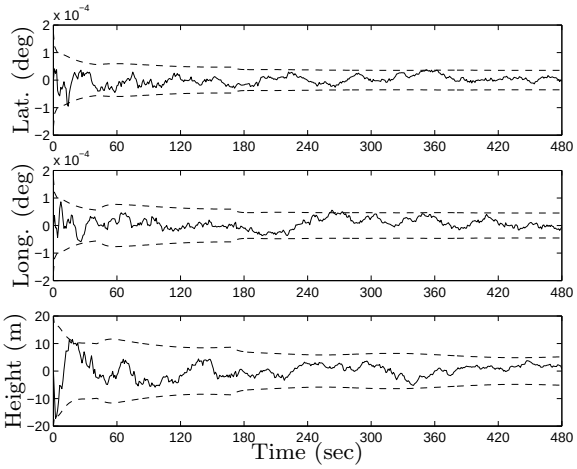

(d) UF Position Errors and 3σ Bounds

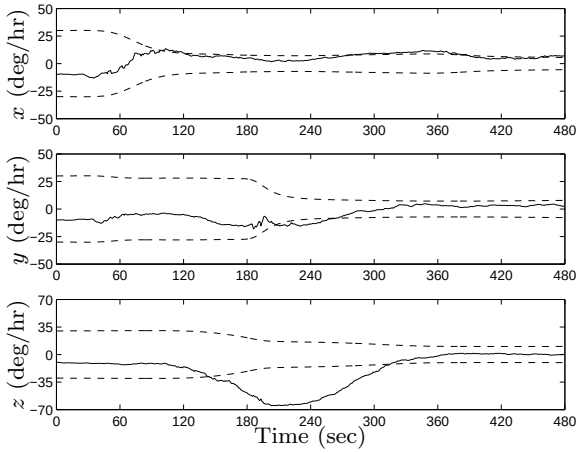

(e) EKF Gyro-Bias Errors and 3σ Bounds

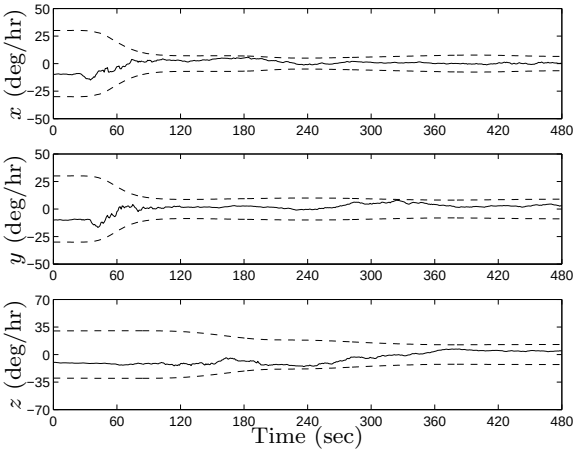

(f) UF Gyro-Bias Errors and 3σ Bounds

Figure 3. EKF and UF Results for Large Initial Errors